NASA TECHNICAL MEMORANDUM

NASA TM X-3012

NASA TM X-3012

(NASA-TM-X-3012) FREQUENCY RESPONSE OF AN AXIAL-FLOW COMPRESSOR EXPOSED TO INLET PRESSURE PERTURBATIONS (NASA) 42 p HC $3.25 CSCL 21E

N74-21398

Unclas

H1/28 36810

FREQUENCY RESPONSE OF AN AXIAL-FLOW COMPRESSOR EXPOSED TO INLET PRESSURE PERTURBATIONS

by Edward J. Milner, Leon M. Wenzel, and Francis J. Paulovich

Lewis Research Center
Cleveland, Ohio 44135

NATIONAL AERONAUTICS AND SPACE ADMINISTRATION • WASHINGTON, D. C. • APRIL 1974

1. Report No.	2. Government Accession No.	3. Recipient's Catalog No.
NASA TM X-3012		

4. Title and Subtitle	5. Report Date
FREQUENCY RESPONSE OF AN AXIAL-FLOW COMPRESSOR EXPOSED TO INLET PRESSURE PERTURBATIONS	APRIL 1974
	6. Performing Organization Code

7. Author(s)	8. Performing Organization Report No.
Edward J. Milner, Leon M. Wenzel, and Francis J. Paulovich	E-7709
	10. Work Unit No. 501-24
9. Performing Organization Name and Address Lewis Research Center National Aeronautics and Space Administration Cleveland, Ohio 44135	11. Contract or Grant No.
	13. Type of Report and Period Covered Technical Memorandum
12. Sponsoring Agency Name and Address National Aeronautics and Space Administration Washington, D. C. 20546	14. Sponsoring Agency Code

15. Supplementary Notes

16. Abstract

Presented are the experimental results of a series of engine tests designed to obtain the stage dynamics of an eight-stage axial-flow compressor over the frequency range of 0.5 to 200 hertz. The total pressure at the compressor face was varied by means of a secondary air jet system installed in the engine inlet and positioned to oppose the primary airflow. Total-pressure probes located at each compressor stage were used to obtain the frequency response of each compressor-stage total pressure to the average compressor-inlet total pressure. The engine operating conditions were chosen to illustrate the effects of changing the rotor speed, changing the exhaust nozzle area, and isolating the compressor discharge pressure perturbations from the fuel control - and hence, the fuel flow.

17. Key Words (Suggested by Author(s))	18. Distribution Statement
Multistage compressor dynamics; Axial compressor; Compressor stage frequency responses; Sweep frequency testing	Unclassified - unlimited CAT. 28

19. Security Classif. (of this report)	20. Security Classif. (of this page)	21. No. of Pages	22. Price*
Unclassified	Unclassified	42	$3.25

* For sale by the National Technical Information Service, Springfield, Virginia 22151

FREQUENCY RESPONSE OF AN AXIAL-FLOW COMPRESSOR EXPOSED TO INLET PRESSURE PERTURBATIONS

by Edward J. Milner, Leon M. Wenzel, and Francis J. Paulovich

Lewis Research Center

SUMMARY

This report presents the experimental results of a series of engine tests designed to obtain the stage dynamics of an eight-stage, axial-flow compressor. The inlet was equipped with a secondary air jet system positioned to oppose the primary airflow. The resultant momentum exchange between the two air streams allowed the total pressure at the compressor face to be varied.

The compressor stages were instrumented with total-pressure probes so that frequency response curves of each stage total pressure to the average compressor-inlet total pressure could be obtained. The engine operating conditions chosen for this study make it possible to examine the effects of changing the rotor speed, changing the exhaust-nozzle area, and isolating the compressor discharge pressure perturbations from the fuel control.

The study revealed that at 87 and 94 percent of rated speed, isolating the compressor discharge pressure perturbations from the fuel control seems to affect the back stages of the compressor, particularly at low frequencies. Changes in the exhaust-nozzle throat area have no apparent effect at 87 percent of rated speed. However, at 94 percent of rated speed, some effect is evident, particularly in the middle stages of the compressor. When rotor speed is increased, resonances and antiresonances become amplified and more pronounced.

INTRODUCTION

The emphasis in the design of air-breathing engines is on high thrust with a minimum of weight. Although many significant steps have been taken in this direction, a continuing trend has been toward the use of lightweight, high-performance multistage compressors. An optimum design would be for each stage of the compressor to operate at or near its maximum efficiency with suitable stall margin as required by the individual stages. However, in order to attain the optimum design, a knowledge of the dynamic stage character-

istics of the compressor is essential.

The experimental results of a series of engine tests designed to obtain the stage-by-stage dynamics of an eight-stage, axial-flow compressor are documented in this report. The inlet was equipped with a secondary air jet system (ref. 1) driven by a high-response servovalve (ref. 2) so that the compressor-inlet total pressure $P_{t,2}$ could be varied in a controlled manner.

The compressor stages were instrumented with total-pressure probes so that frequency characteristics of each stage total pressure $P_{t,2.i}$ could be obtained. Compressor-stage dynamics are presented for several different engine operating conditions. The operating conditions chosen for this study allow an examination of the effects of changing the rotor speed, changing the exhaust nozzle area, and isolating the compressor discharge pressure perturbations from the fuel control. The effect of each of these parameters on the stage dynamics of the compressor is discussed in this report.

SYMBOLS

A area, cm^2

N percent of rated engine speed (16 500 rpm)

P pressure, N/cm^2

Subscripts:

c corrected

t total

1 airflow measuring station at bell-mouthed inlet

2 compressor inlet measuring station

2.i i^{th} compressor stage exit measuring station

3 compressor discharge measuring station

8 exhaust nozzle throat station

Superscript:

$\overline{(\,)}$ denotes mean value

APPARATUS AND PROCEDURE

Tests were conducted with a General Electric J85-13 turbojet engine in an altitude chamber. The inlet of the engine used was equipped with a secondary air jet system

(ref. 1).

Eighteen (18) secondary air nozzles were spaced over a cross section of the inlet duct. Each was positioned so that the airflow from the jet nozzle would oppose the primary inlet flow. The resultant momentum exchange between the two opposing air streams causes a total pressure loss across the jets which thus allows the total pressure at the compressor face to be varied.

A sweep oscillator was used to generate a sinusoidal signal whose frequency varied logarithmically with time. An analog computer was used to condition this signal, thereby allowing an operator to vary its amplitude. The sinusoidal signal was connected to a high-response servovalve (ref. 2) which in turn controlled the airflow to the 18 air-jet nozzles located in the engine inlet.

The General Electric J85-13 turbojet engine has an eight-stage axial-flow compressor equipped with three controlled innerstage bleeds. The compressor is directly coupled to a two-stage turbine. The engine also has an afterburner section and an exhaust nozzle with a variable throat area. The combustor is a through-flow annular type. Figure 1 presents a schematic of the engine along with the secondary air jet system.

Located in the engine inlet are variable guide vanes which are mechanically linked to the interstage bleeds in such a way that the bleeds will be fully open when the inlet guide vanes are positioned at their maximum angle. For this study, the interstage bleeds were scheduled to be fully open below 78 percent corrected speed and to be fully closed above 92 percent corrected speed. The turbine diaphragm area was 232 square centimeters. The reduced turbine diaphragm area was needed for other tests in this series which required the compressor to be stalled without exceeding maximum temperature limits.

Normally, during engine operation the compressor-discharge static pressure is sensed by the fuel control. This type of test is designated in table I as an "untrapped P_3" case. To investigate the effects of P_3-induced fuel-flow perturbations, P_3 perturbations were isolated from the fuel control by means of a solenoid valve. These tests are referred to as "trapped P_3" tests.

Instrumentation

The engine compressor was instrumented with 17 high-response total-pressure transducers as shown in figure 2. The frequency characteristics of the transducers and probes were essentially flat to 400 hertz.

Only the transient characteristics of each data signal were of interest in this program. To obtain these responses, each transducer output was biased to remove its dc or steady-state, portion. In addition, an appropriate gain was selected to give the resulting transient response a reasonable signal level. Since the values changed from test to test, it was necessary to rezero each of the transducers and to calibrate the gain prior

to each test. To manually do this would be time consuming, especially since the engine must be operating during the calibration.

A system (Sum and Buck Unit) was developed at the Lewis Research Center to automatically zero each transducer immediately prior to the start of a test. With the engine operating at the test condition, the compressor-inlet total-pressure $P_{t,2}$ is exposed to a very low frequency sinusoidal variation. The Sum and Buck Unit then cycles through each data signal and obtains its steady-state value. An appropriate bias voltage proportional to this steady-state value is added to the transducer signal to buck out the dc part of the data signal. The Sum and Buck Unit also allows the gain of each transducer to be set quickly, so that a signal with a reasonable level can be recorded. By monitoring each data signal on an oscilloscope, one can amplify or attenuate a signal by simply adjusting a multi-position switch. The zeroing and gain-setting operations can be accomplished readily, so that the test can be completed and the data obtained before zero drift occurs in the transducers.

In addition to the dynamic data system that has been described, a second data system was also provided to measure steady-state levels. A pressure tap was provided at each transducer location. The pressure taps were connected to a very accurate data system (ref. 3) for measuring the steady-state pressure at each location.

Test Procedure

The investigation was conducted by applying a sinusoidal variation in total pressure at the compressor face. The frequency of the perturbation was varied logarithmically with time to allow the use of the sweep frequency test techniques of references 4 and 5.

The airflow through the valve used to control the air-jet system is a function of the stroke of the valve. Figure 3 shows the pressure gradient between the bell-mouthed inlet and the compressor face $(P_{t,1} - P_{t,2})$ as a function of valve stroke. During a test, it is desirable to have the valve operating on the linear portion of the curve. At the beginning of each test, the valve position and the bell-mouthed-inlet total pressure $P_{t,1}$ were adjusted to satisfy this condition for the compressor-face total pressure desired.

The test procedure was as follows. A steady-state engine operating condition was established for the desired rotor speed and exhaust nozzle area. The steady-state compressor-inlet pressure and temperature were chosen to be 6.9 newtons per square centimeter, and approximately 295 K, respectively. A sweep-frequency oscillator was used to generate a sinusoidal signal with a constant frequency of 0.5 hertz. This signal was connected to a table-top analog computer. The output of the computer was used to drive the high-response servovalves to control tne air-jet system. The amplitude of the valve stroke was adjusted to obtain a peak-to-peak perturbation of 0.69 newton per square centimeter in the total pressure $P_{t,2}$ at the compressor face. When the adjust-

ments were completed, the sweep-frequency oscillator was put into the sweep mode, and a sinusoidal disturbance was generated. A sweep rate of one decade per minute was maintained (ref. 4).

For each of these tests, the desired frequency range was 0.5 to 200 hertz. The first sweep of each test was used to assure that this frequency range could be swept without the compressor stalling. If no stall occurred, the sweep test was then repeated. During the second sweep, the sinusoidal signal used to drive the servovalve, its corresponding quadrature signal (which is also generated by the sweep frequency oscillator), and the output of each of the 17 total-pressure transducers were recorded on a 42 channel frequency-modulated tape recorder.

If the compressor did stall during the initial sweep test, the amplitude of the valve stroke (and, thus, the amplitude of the $P_{t,2}$ perturbation) was decreased slightly, so that the entire sweep range could be completed. This procedure was followed for each of the tests summarized in table I. In order to complete the sweep test for 100 percent of rated speed, the amplitude of the $P_{t,2}$ signal was necessarily very small.

The recorded raw data were processed with the use of a general-purpose hybrid computer. The technique used (ref. 5) obtains the frequency, magnitude, and phase of each data channel. These results were then used to obtain frequency-response plots of the ratio of each compressor-stage pressure to the compressor-inlet pressure.

RESULTS AND DISCUSSION

The operating conditions for these tests were chosen so that the resulting sweep data could be used to demonstrate the effects on the engine characteristics of trapping the compressor discharge pressure perturbations, changing the exhaust-nozzle area, and changing the rotor speed. Each of these will be discussed separately.

Effect of Trapping the Compressor Discharge Pressure Perturbations

Trapped and untrapped sweeps at corrected speed of 87 percent rated (N_c = 87 percent) and an exhaust nozzle area A_8 of 735 square centimeters are compared for each stage in figures 4 and 5. The frequency responses of the ratios of the stage pressures $P_{t,2,i}$ to the average pressure $\overline{P}_{t,2}$ at the compressor face for the trapped and untrapped conditions are essentially the same for the $\overline{P}_{t,2}$ values and exhibit similar characteristics for the first six stages of the compressor. In stage 7, though, particularly in the frequency range of 2 to 80 hertz, the gain with the trapped condition is slightly higher than with the untrapped condition. At compressor discharge, there is still higher gain in the frequency range of 2 to 80 hertz for the trapped case.

Trapped and untrapped sweeps for N_c = 94 percent and A_8 = 735 square centimeters are compared in figures 6 and 7. For these sweep tests, one observes similar effects as were noted for the corresponding data with N_c = 87 percent. Hence, the effects of trapping do not seem to be influenced by rotor speed in these two cases.

At 100 percent of rated speed, the raw data had to be recorded at such a low signal level that the resulting frequency-response plots have enough scatter to mask any change that may occur between the trapped and untrapped sweeps.

Exhaust-Nozzle-Area Effects

A comparison of the trapped sweep data at 87 percent of rated speed for exhaust nozzle areas of 735 and 626 square centimeters (figs. 4 and 8, respectively) shows that the corresponding frequency responses of the ratios of each stage pressure $P_{t,\,2.i}$ to the average inlet pressure $\overline{P}_{t,\,2}$ are essentially the same. Likewise, a comparison of the untrapped sweep data at 87 percent of rated speed for exhaust nozzle areas of 735 and 626 square centimeters (figs. 5 and 9, respectively) shows that the corresponding frequency responses of $P_{t,\,2.i}/\overline{P}_{t,\,2}$ are similar.

A comparison of the trapped sweep data at 94 percent of rated speed for exhaust nozzle areas of 735 and 677 square centimeters (figs. 6 and 10, respectively) shows that the frequency responses of $P_{t,\,2.i}/\overline{P}_{t,\,2}$ are again similar, except for stages 3 and 4 at very low frequencies. There is a slight mismatch in the frequency-response curves of $P_{t,\,2.3}/\overline{P}_{t,\,2}$ at frequencies below 3 hertz, where the curve for the 677-square-centimeter exhaust-nozzle area is shifted down slightly. The same mismatch is evident in the frequency-response curves of $P_{t,\,2.4}/\overline{P}_{t,\,2}$, but it occurs at frequencies below 6 hertz.

Comparing the sweep for A_8 = 626 square centimeters (fig. 11) with that for A_8 = 735 square centimeters (fig. 6) reveals that the attenuation characteristics have the same general shape. However, some differences also occur. The $\overline{P}_{t,\,2}$ curves show an organ-pipe effect. The resonance at 80 hertz for the 626-square-centimeter nozzle area is lower than that for the 735-square-centimeter nozzle area. At stage 3, although the corresponding frequency-response curves have similar characteristics, there is some mismatch in the frequency range of 30 to 125 hertz that is due to the deeper antiresonance at about 50 hertz for the 735-square-centimeter nozzle area. These same effects are evident in the curves for stages 4, 5, and 7. At both stage 6 and the compressor exit (station 3), there is a slightly lower attenuation in the 626-square-centimeter curves for the frequency range of 30 to 90 hertz.

At 100 percent of rated speed, it is not feasible to compare the corresponding frequency responses at different exhaust nozzle areas. The low signal-to-noise ratio at this

speed causes enough scatter in the frequency-response curves to make the results of such a comparison uncertain. It is not certain whether the differences between the corresponding frequency responses are due to the exhaust nozzle areas or whether it is just scatter due to the low signal level at this speed.

Rotor-Speed Effects

The results of the sweep frequency tests for an exhaust nozzle area of 735 square centimeters and untrapped P_3 are compared for rotor speeds of 87, 94, and 100 percent of rated speed (figs. 5, 7, and 12). An overall observation that can be made in comparing these frequency responses for $P_{t,2.i}/P_{t,2}$ is that, in general, the shapes of the corresponding curves are essentially the same at corrected speeds of 87 and 94 percent. However, the resonances and antiresonances are much more pronounced in the corresponding frequency responses for the 94-percent than for the 87-percent speed.

A stage-by-stage examination of each of these sweeps reveals that at 87-percent corrected speed (fig. 5), the curve is essentially flat for the first stage of the compressor. The characteristics for stages 2, 3, and 4 form small peaks at about 18 hertz and then decrease between 30 and 125 hertz. Stage 5 forms a small peak at 35 hertz in addition to the peak at 18 hertz. These two peaks are also found throughout the remainder of the compressor. The stage-5 curve also shows a small valley at about 100 hertz which transforms in stage 6 to a medium-size antiresonance at about 90 hertz. In stages 7 and 8, the frequency of this antiresonance shifts to about 125 hertz.

For a rotor speed of 94 percent of rated speed (fig. 7), the stage-1 curve has an antiresonance at 30 hertz, with the remainder of the curve being essentially flat. However, in stage 2 it is reflected into a huge antiresonance. This antiresonance decreases in compressor stages 3 and 4 and occurs about 50 hertz. These stages also develop a resonance at about 18 hertz which follows through stages 5, 6, and 7 and finally develops into a large resonance in stage 8. Stage 5 develops a small peak at about 35 hertz that is visible throughout the remaining compressor stages. This stage also has a large valley between 40 and 100 hertz, which becomes a medium-size antiresonance at about 90 hertz in stage 6. In stage 7, this effect becomes a large antiresonance in the range of 60 to 100 hertz, but it shifts its frequency to about 125 hertz in stage 8.

At rated speed (fig. 12), the stage-1 curve shows a sharp, deep valley at about 20 hertz, with the rest of the curve being essentially flat. A slight dip between 5 and 10 hertz develops in stage 2 which is amplified to a medium-size depression between 3 and 7 hertz in stages 3 and 4. Also, the stage-2 curve shows a medium-size resonance at about 20 hertz which is also visible in stages 3 and 4. In stage 5, the resonance of the previous three stages becomes a huge antiresonance at about 23 hertz. The remainder of

the curve is flat, but its normalized magnitude is only 0.5. Stage 6 shows a small peak at about 18 hertz, and then the curve rolls off sharply. However, a large resonance extends from 25 to 100 hertz. The stage-7 resonance at about 18 hertz and the antiresonance between about 30 and 150 hertz develop in stage 8 into a huge resonance at about 18 hertz and an antiresonance at about 50 hertz.

Figure 13 shows typical stage frequency responses obtained from a J85 engine simulation described in reference 6. In this simulation model, fuel flow is kept fixed at its steady-state value. The results presented correspond to the engine conditions of figure 8. For actual engine tests, there appear to be differences in the higher frequency range that are not accounted for in the simulation model.

SUMMARY OF RESULTS

Tests were conducted with a General Electric J85-13 turbojet engine in an altitude chamber. Operating conditions were chosen to study the effects on the engine characteristics of (1) isolating the compressor discharge pressure perturbations from the fuel control (i.e., trapping the compressor discharge pressure perturbations), (2) exhaust nozzle area, and (3) rotor speed. The stage dynamics of the compressor were obtained in the form of frequency-response plots. Comparisons of corresponding frequency responses at the different engine operating conditions indicated the following principal results:

1. The corresponding frequency responses for trapped and untrapped sweeps were examined at 87 and 94 percent of rated speed. At each of these speeds, the response characteristics for the last three compressor stages of the trapped case have higher gain than those of the untrapped case for the frequency range of interest. The magnitude of this change in gain seems to be independent of rotor speed.

2. There is no apparent exhaust-nozzle-area effect at 87 percent of rated speed. The corresponding frequency response curves for sweeps with different exhaust nozzle throat areas are similar at this speed. However, a comparison of sweeps with different throat areas at 94 percent of rated speed shows that although the corresponding curves have the same basic shape, some mismatch does occur, particularly in the middle stages of the compressor.

3. In general, the shapes of the corresponding frequency-response curves are essentially the same at rotor speeds of 87 and 94 percent of rated speed. However, resonances and antiresonances occurring for the 87-percent speed are much more pronounced

for the corresponding condition at the 94-percent speed. These effects are greatly amplified for the corresponding frequency responses at 100 percent of rated speed.

Lewis Research Center,
National Aeronautics and Space Administration,
Cleveland, Ohio, November 9, 1973,
501-24.

REFERENCES

1. Meyer, Carl L.; McAulay, John E.; and Biesiadny, Thomas J.: Technique for Inducing Controlled Steady State and Dynamic Inlet Pressure Distrubances for Jet Engine Tests. NASA TM X-1946, 1970.
2. Baumbick, Robert J.: Device for Producing Dynamic Distortion Patterns at Inlets of Air-Breathing Engines. NASA TM X-2026, 1970.
3. Mealey, Charles; and Kee, Leslie: A Computer-Controlled Central Digital Data Acquisition System. NASA TN D-3904, 1967.
4. Drain, Daniel I.; Bruton, William M.; and Paulovich, Francis J.: Airbreathing Propulsion System Testing Using Sweep Frequency Techniques. NASA TN D-5485, 1969.
5. Milner, Edward J.; and Bruton, William M.: Application of a Hybrid Computer to Sweep Frequency Data Processing. NASA TM X-2753, 1973.
6. Seldner, Kurt; Mihaloew, James R.; and Blaha, Ronald J.: Generalized Simulation Technique for Turbojet Engine System Analysis. NASA TN D-6610, 1972.

TABLE I. - ENGINE CONDITIONS USED FOR SWEEP FREQUENCY TESTS

Percent corrected engine speed, N_c	Exhaust-nozzle throat area, A_8, cm^2	Compressor discharge pressure, P_3	Figure
87	735	Trapped	4
87	735	Untrapped	5
87	626	Untrapped	9
87	626	Trapped	8
94	735	Trapped	6
94	735	Untrapped	7
94	626	Trapped	11
94	677	Trapped	10
100	735	Untrapped	12
100	735	Trapped	--
100	658	Trapped	--

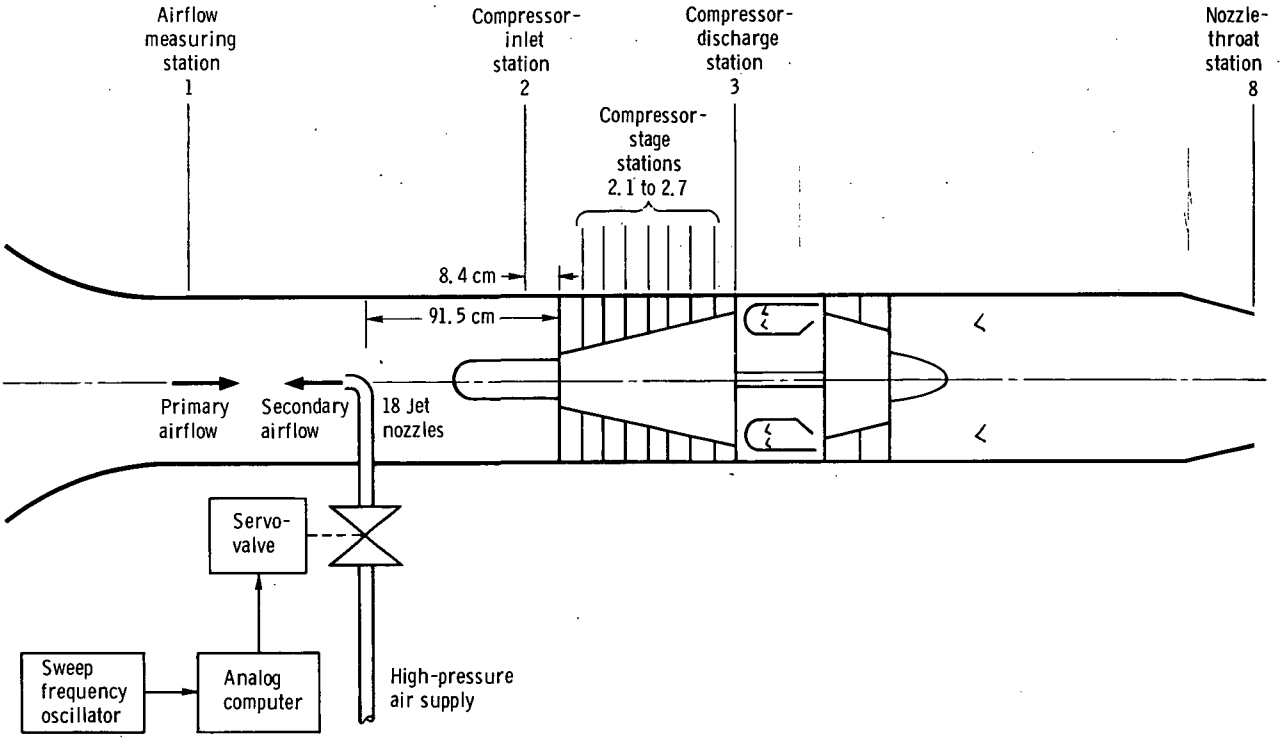


Figure 1. - Schematic diagram of General Electric J85-13 turbojet engine with secondary air-jet system.

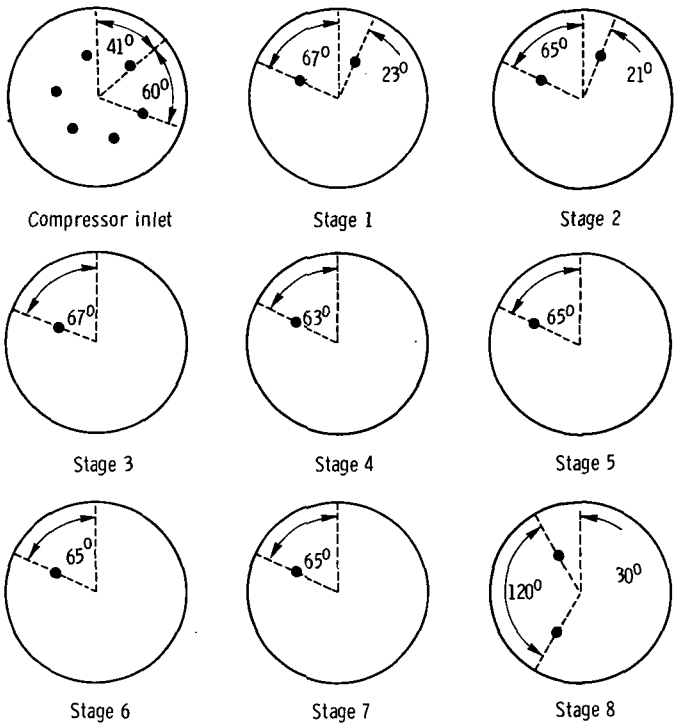


Figure 2. - Locations of total-pressure transducers in compressor stages. View looking upstream. All transducers positioned at midspan.

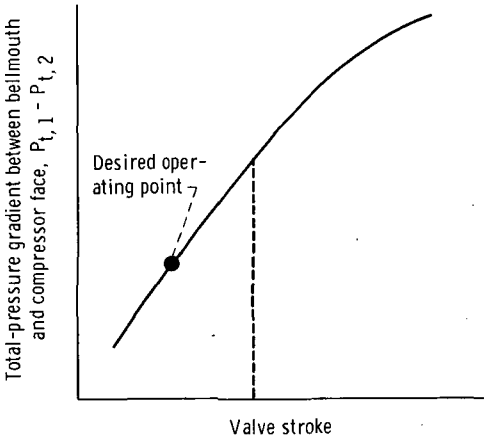
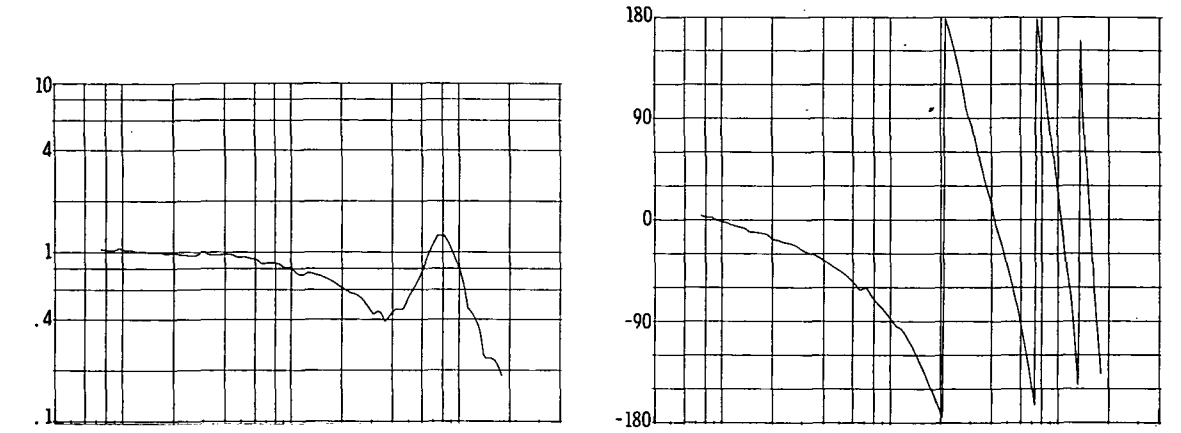
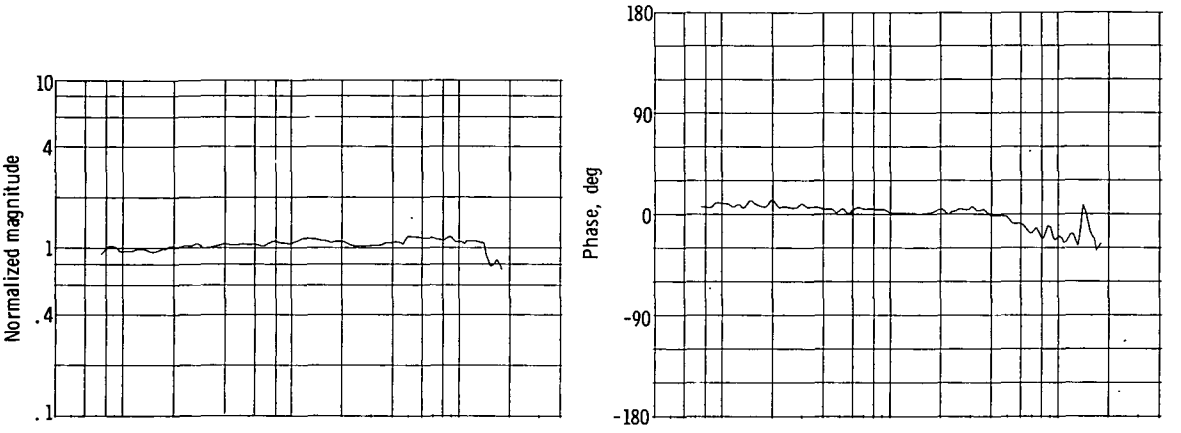


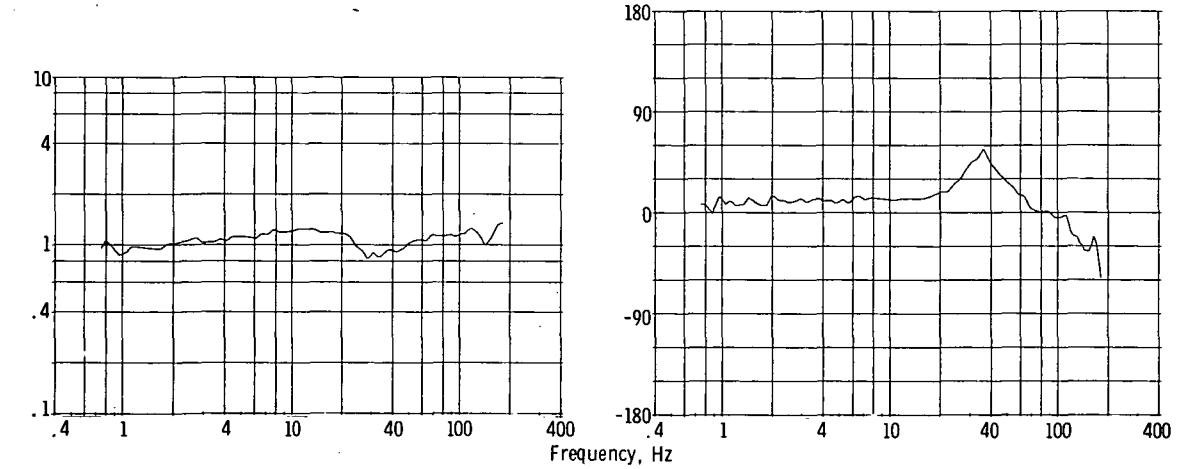
Figure 3. - Total-pressure gradient between bellmouth and compressor face as a function of valve stroke.



(a) Average compressor-face total pressure ($\bar{P}_{t,2}$/ref.).

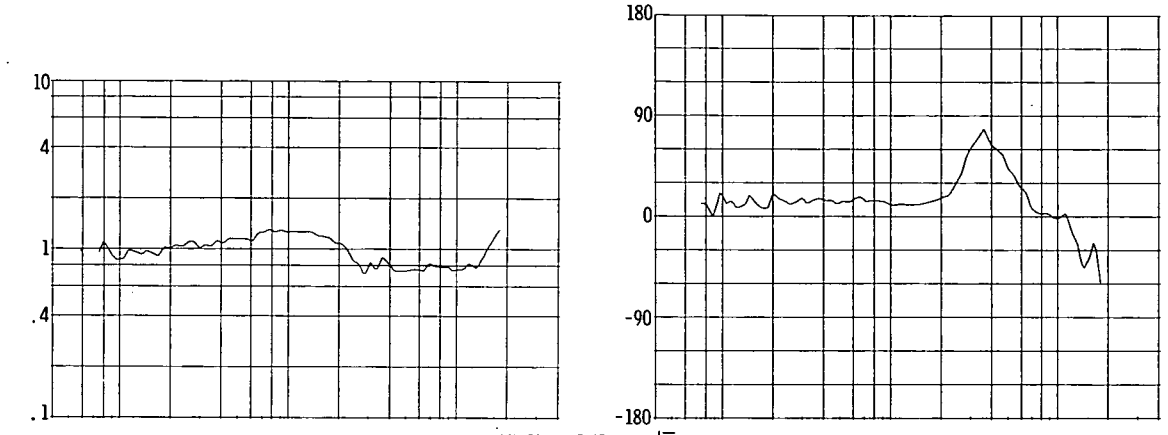


(b) Stage 1 ($P_{t,2.1}/\bar{P}_{t,2}$).

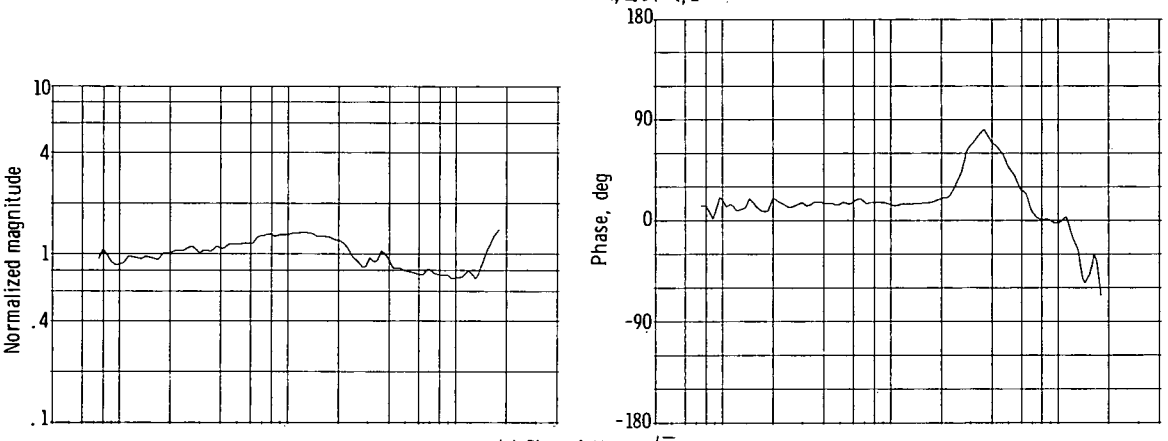


(c) Stage 2 ($P_{t,2.2}/\bar{P}_{t,2}$).

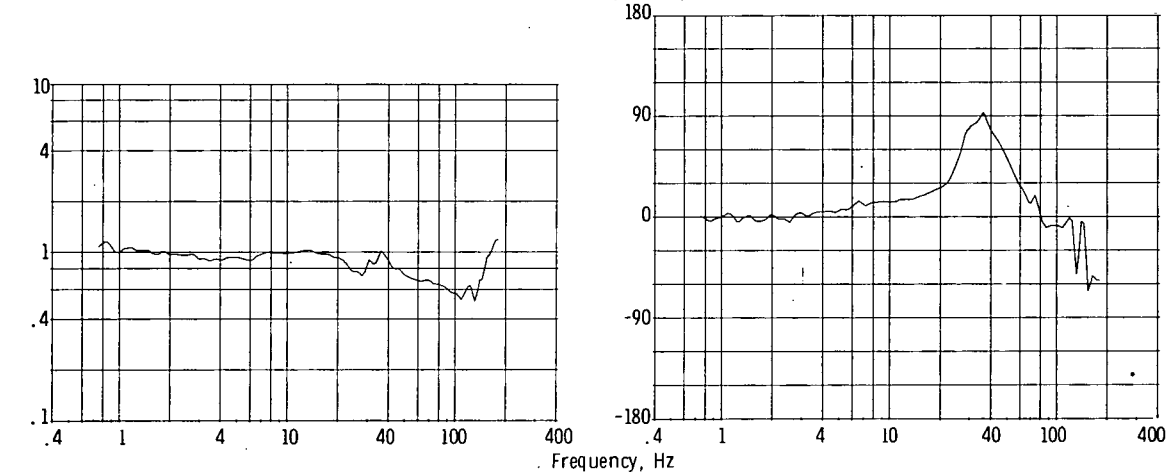
Figure 4. - Normalized frequency responses of engine parameters corresponding to test conditions of 87-percent corrected engine speed, 735-square-centimeter exhaust-nozzle throat area, and trapped compressor-discharge pressure.



(d) Stage 3 ($P_{t,2.3}/\bar{P}_{t,2}$).

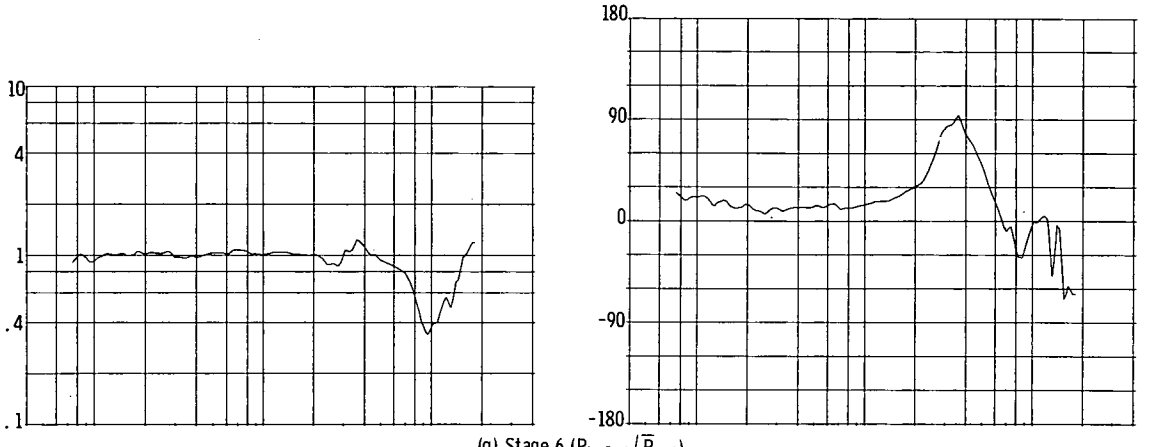


(e) Stage 4 ($P_{t,2.4}/\bar{P}_{t,2}$).

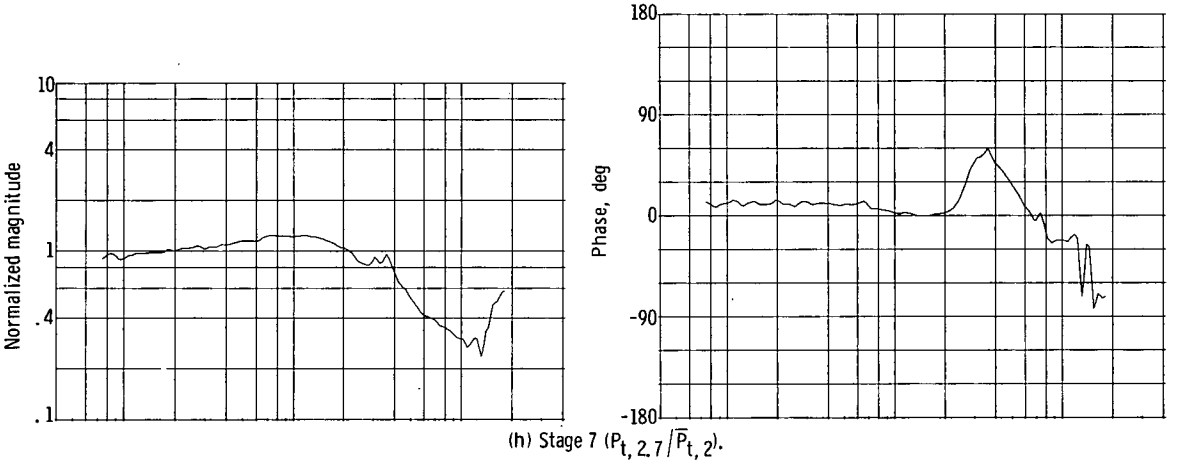


(f) Stage 5 ($P_{t,2.5}/\bar{P}_{t,2}$).

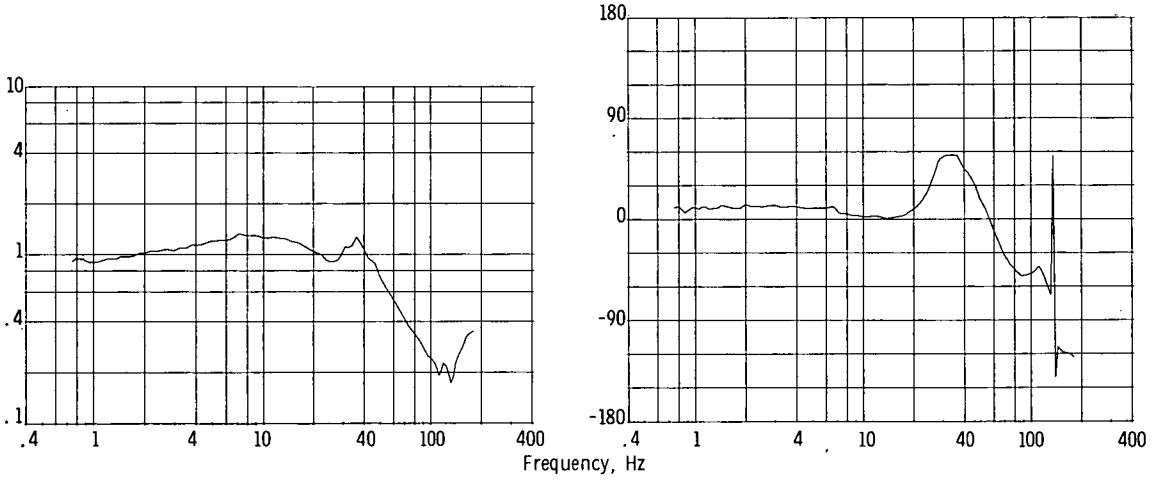
Figure 4. - Continued.



(g) Stage 6 ($P_{t,2.6}/\bar{P}_{t,2}$).

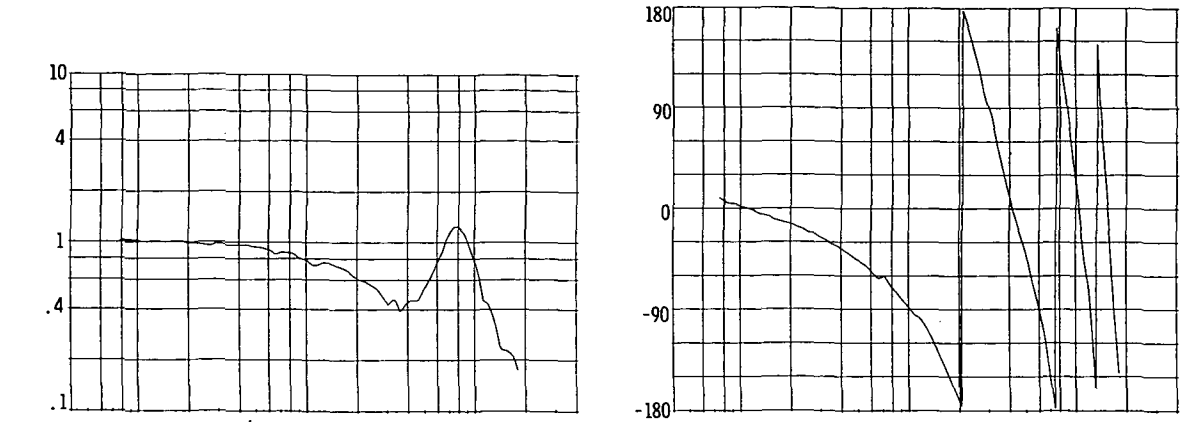


(h) Stage 7 ($P_{t,2.7}/\bar{P}_{t,2}$).

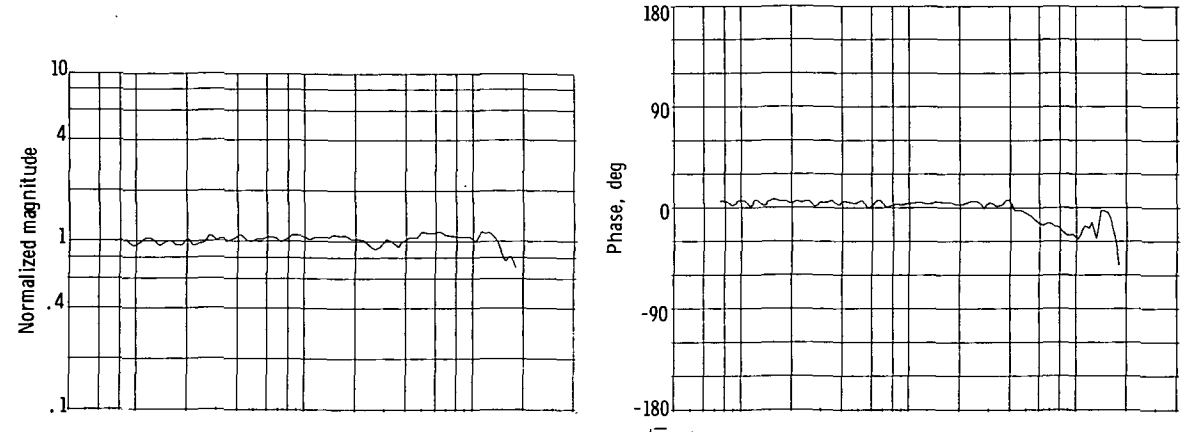


(i) Stage 8 ($P_{t,3}/\bar{P}_{t,2}$).

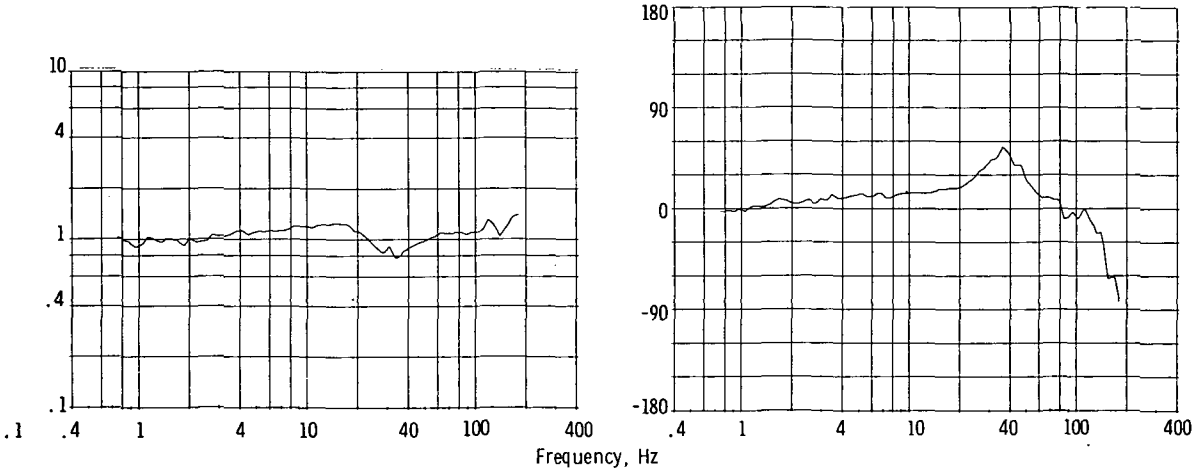
Figure 4. - Concluded.



(a) Average compressor-face total pressure ($\overline{P}_{t,2}$/ ref.).

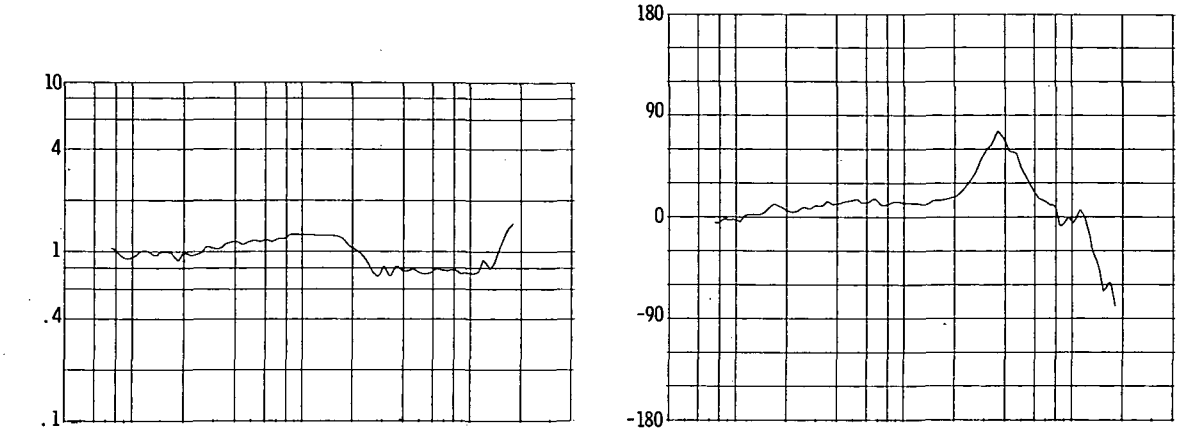


(b) Stage 1 ($P_{t,2.1}/\overline{P}_{t,2}$).

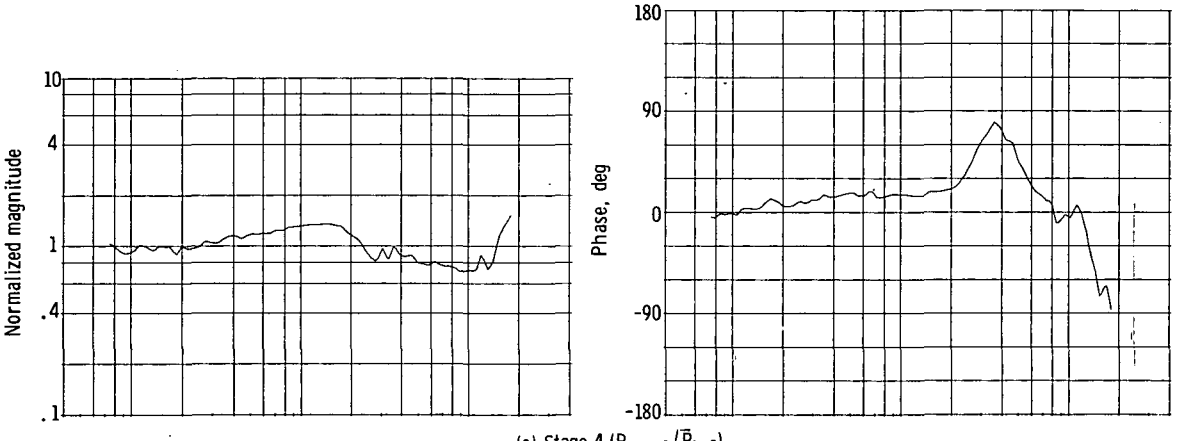


(c) Stage 2 ($P_{t,2.2}/\overline{P}_{t,2}$).

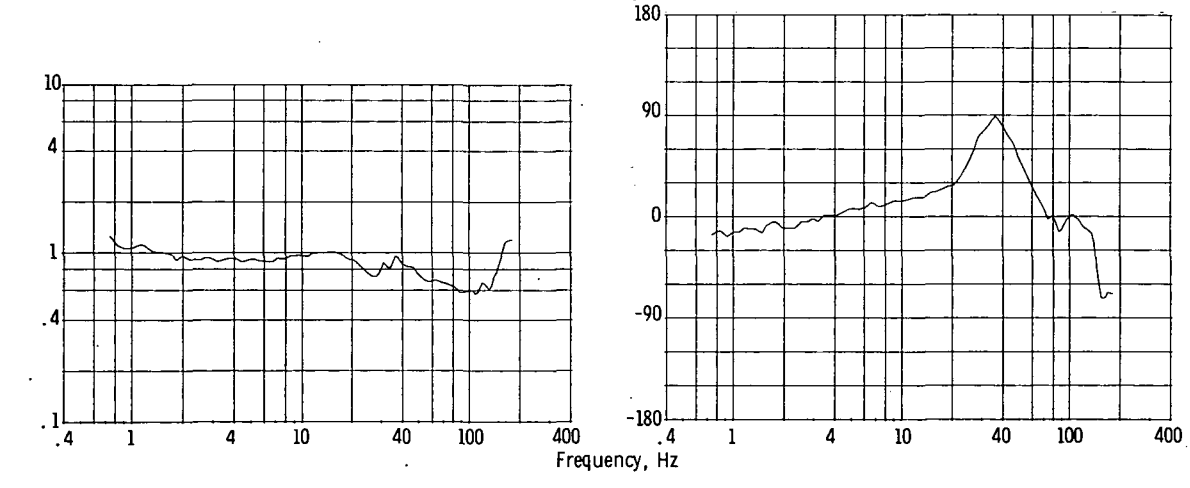
Figure 5. - Normalized frequency responses of engine parameters corresponding to test conditions of 87-percent corrected engine speed, 735-square-centimeter exhaust-nozzle throat area, and untrapped compressor-discharge pressure.



(d) Stage 3 ($P_{t,2.3}/\bar{P}_{t,2}$).

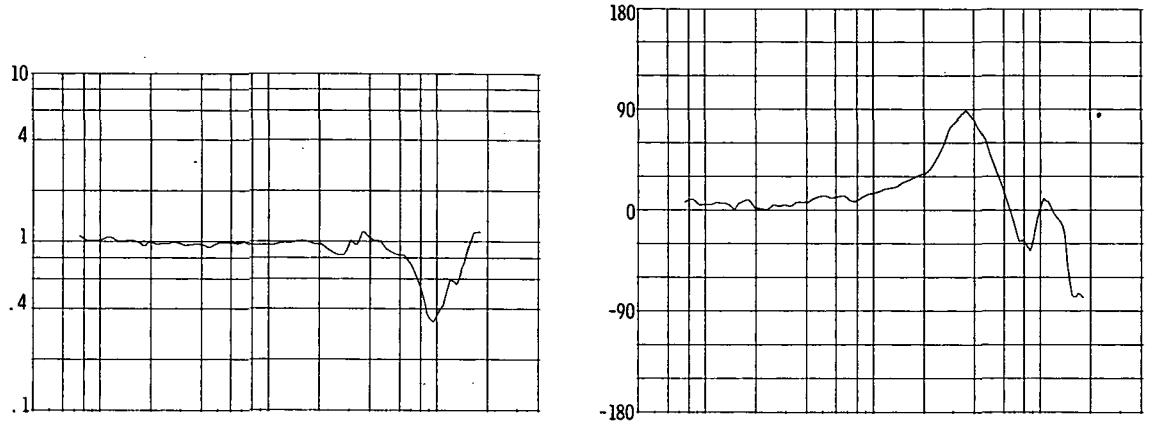


(e) Stage 4 ($P_{t,2.4}/\bar{P}_{t,2}$).

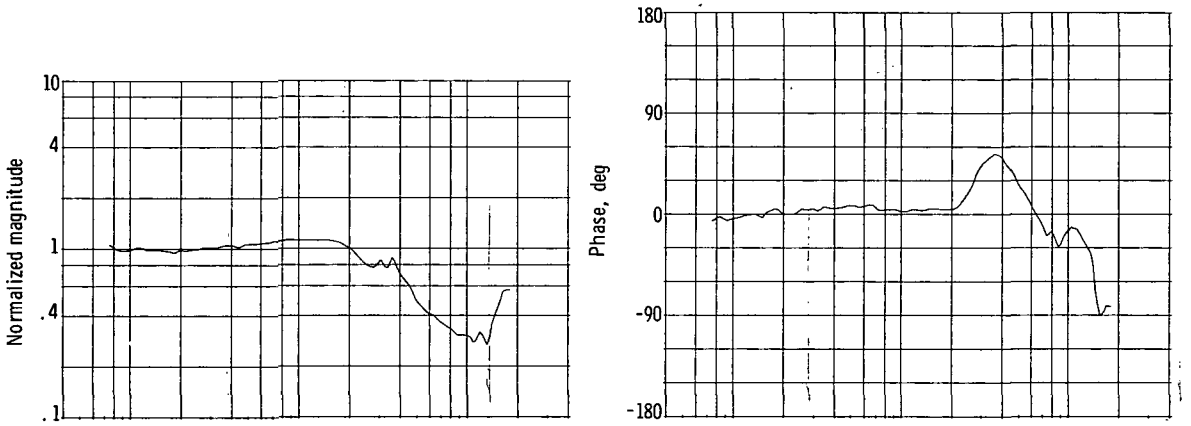


(f) Stage 5 ($P_{t,2.5}/\bar{P}_{t,2}$).

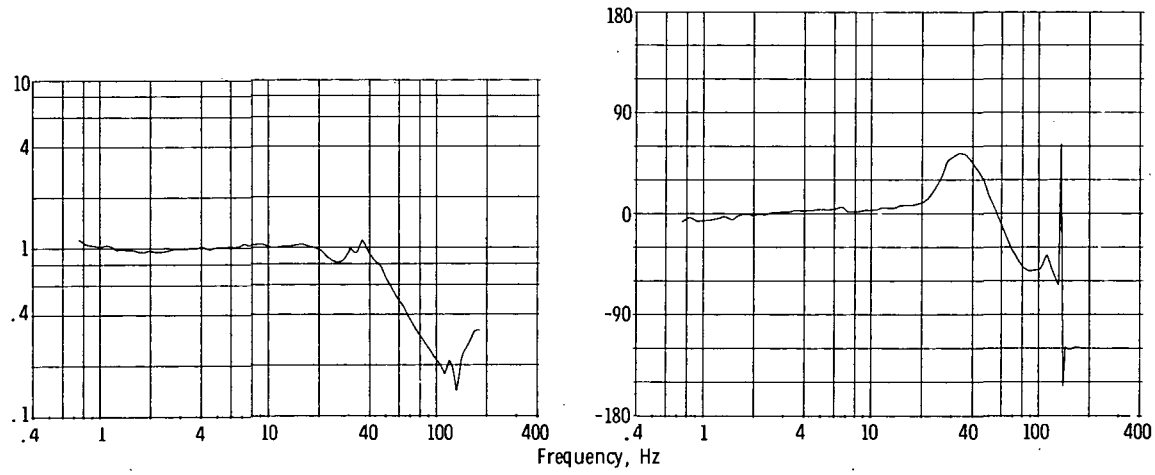
Figure 5. - Continued.



(g) Stage 6 ($P_{t,2.6}/\bar{P}_{t,2}$).

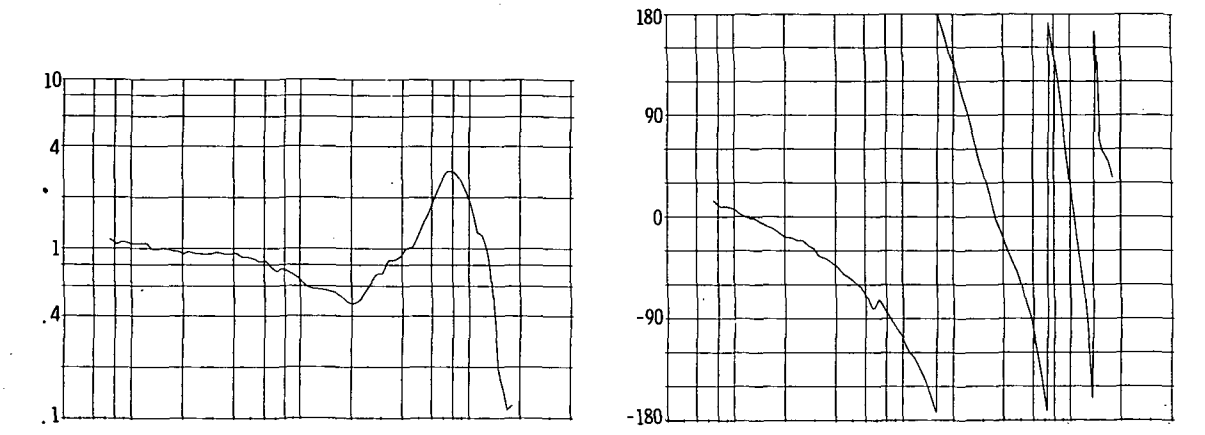


(h) Stage 7 ($P_{t,2.7}/\bar{P}_{t,2}$).

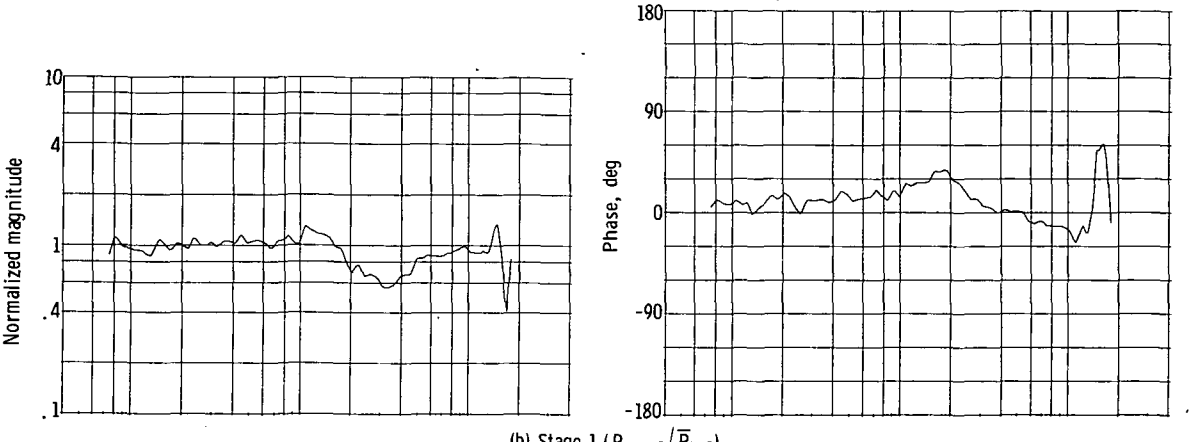


(i) Stage 8 ($P_{t,3}/\bar{P}_{t,2}$).

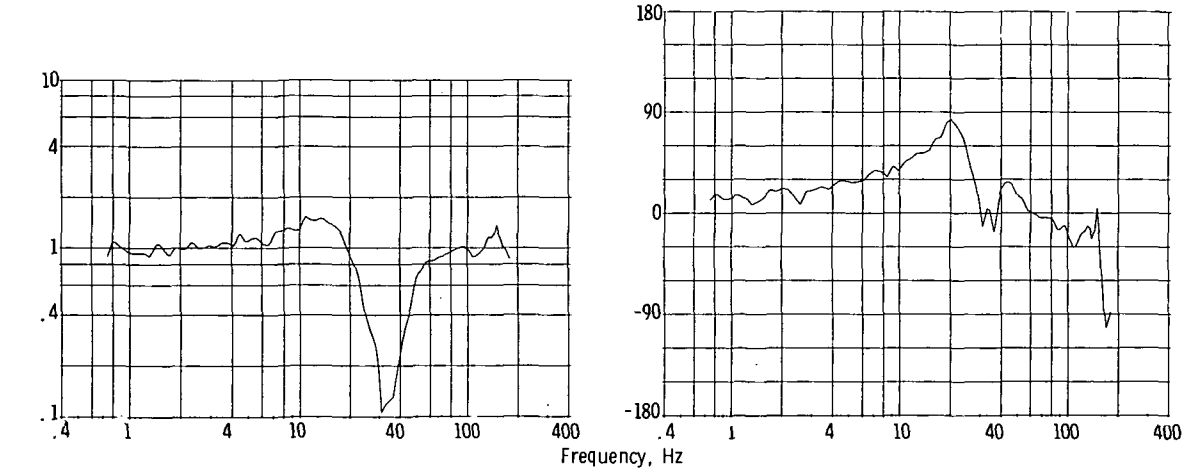
Figure 5. - Concluded.



(a) Average compressor-face total pressure ($\bar{P}_{t,2}$/ref.).

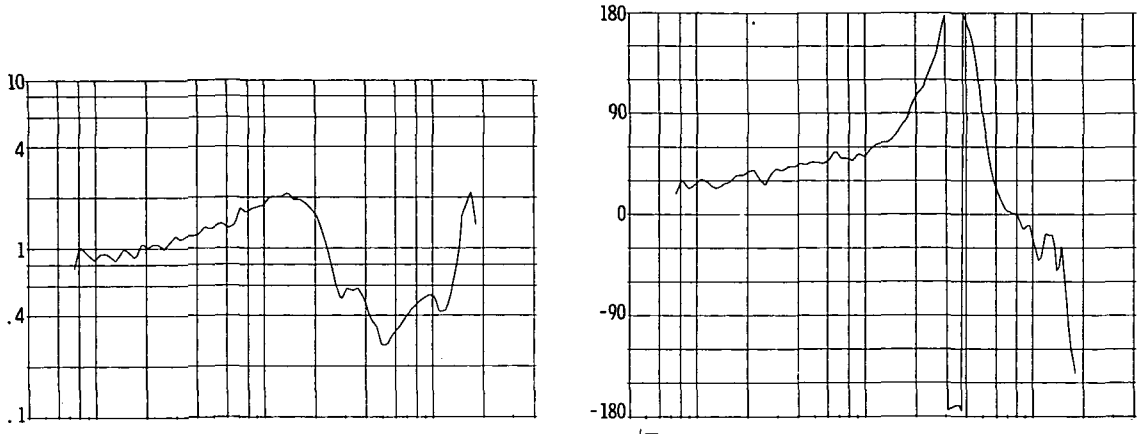


(b) Stage 1 ($P_{t,2.1}/\bar{P}_{t,2}$).

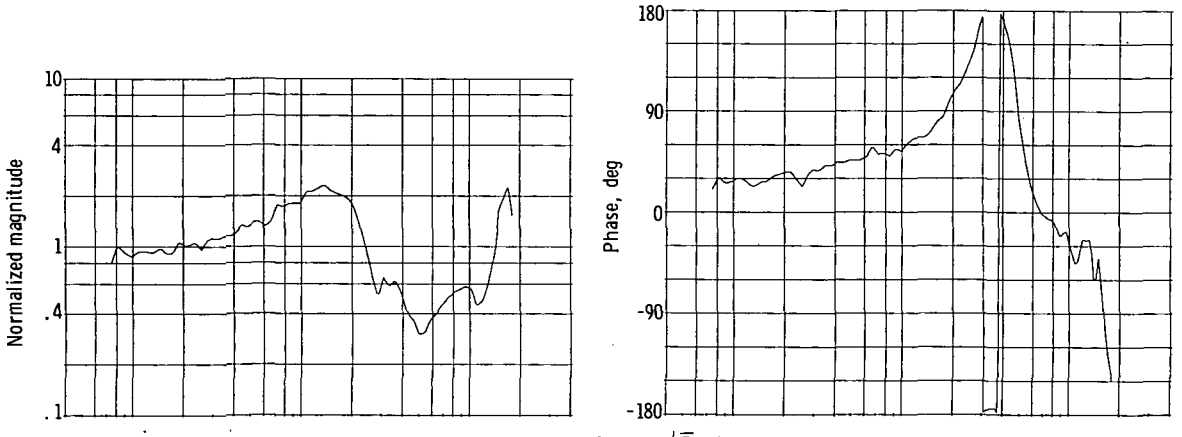


(c) Stage 2 ($P_{t,2.2}/\bar{P}_{t,2}$).

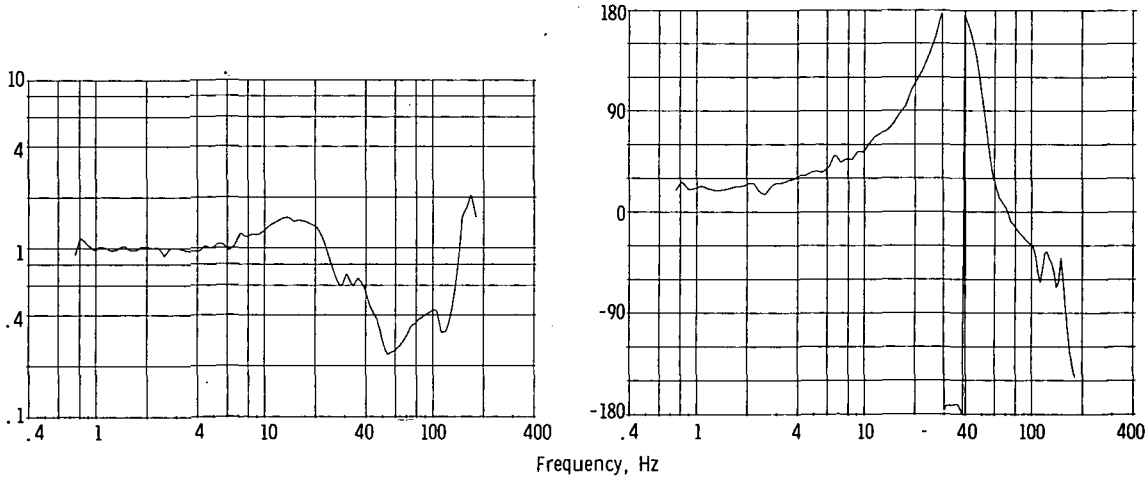
Figure 6. - Normalized frequency responses of engine parameters corresponding to test conditions of 94-percent corrected engine speed, 735-square-centimeter exhaust-nozzle throat area, and trapped compressor-discharge pressure.



(d) Stage 3 ($P_{t,2.3}/\bar{P}_{t,2}$).

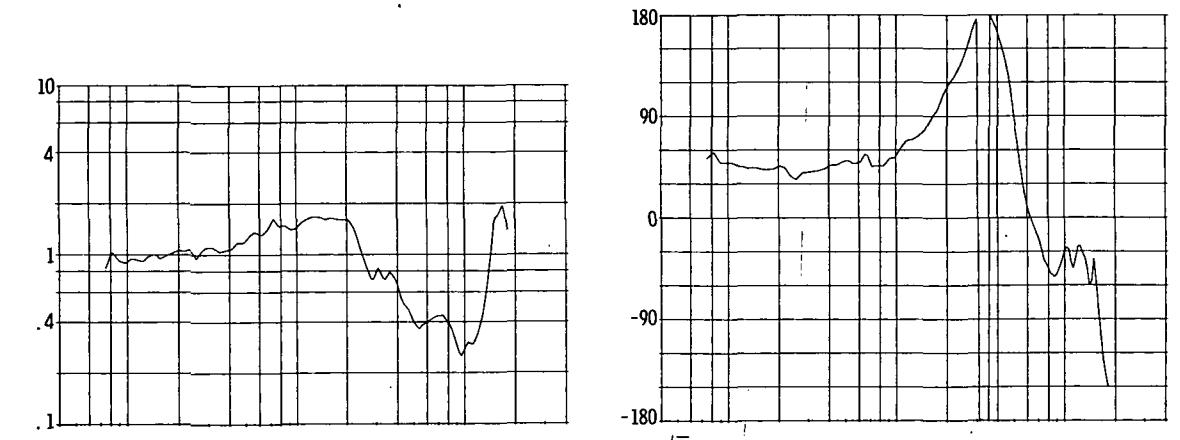


(e) Stage 4 ($P_{t,2.4}/\bar{P}_{t,2}$).

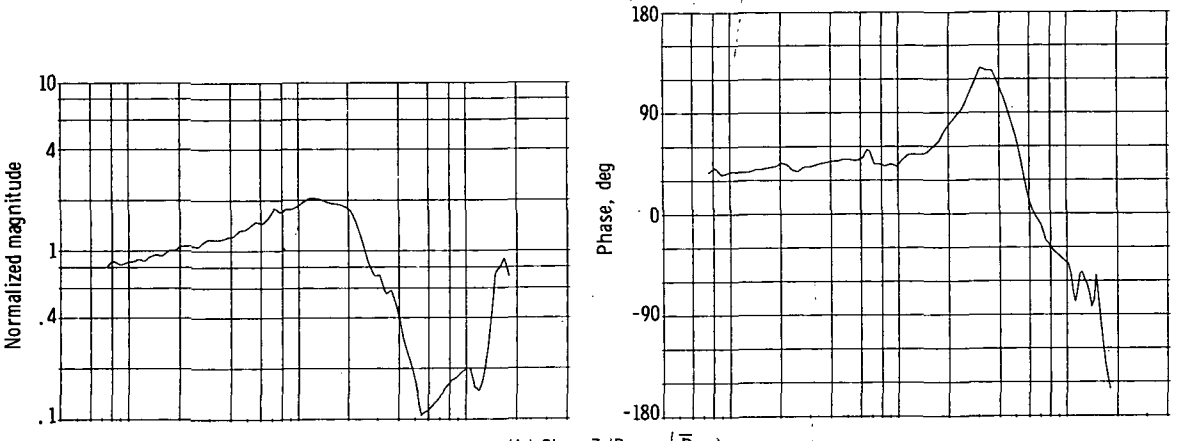


(f) Stage 5 ($P_{t,2.5}/\bar{P}_{t,2}$).

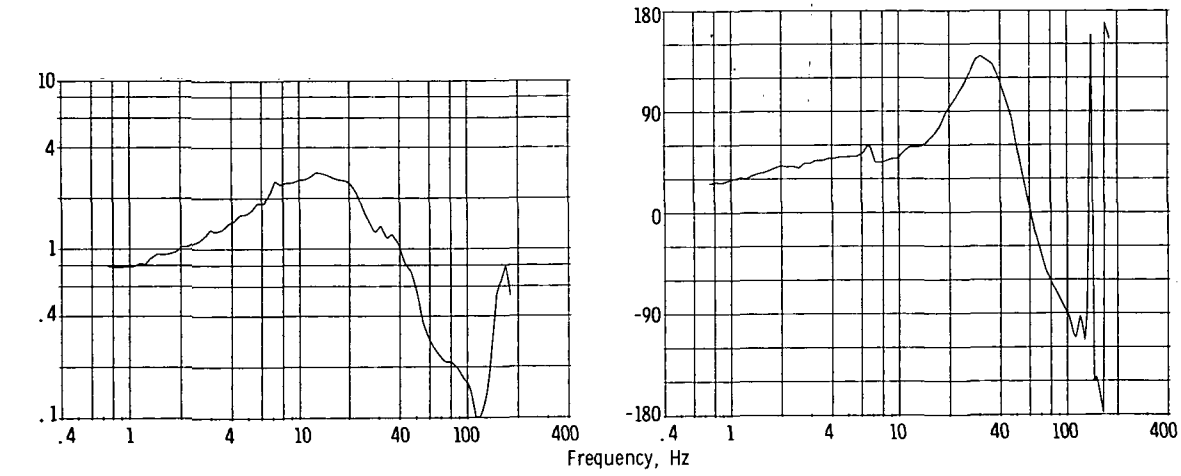
Figure 6. - Continued.



(g) Stage 6 ($P_{t,2.6}/\overline{P}_{t,2}$).

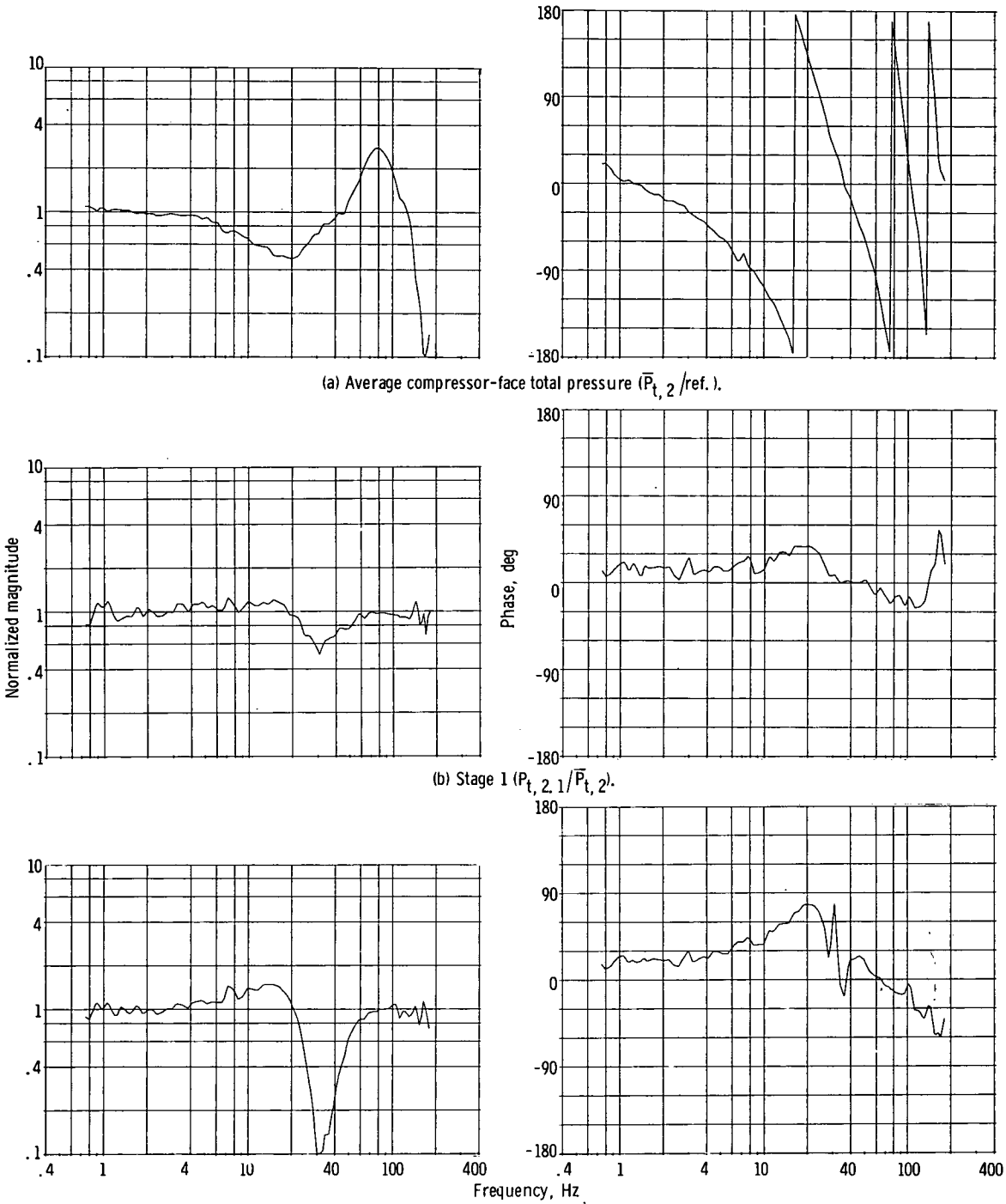


(h) Stage 7 ($P_{t,2.7}/\overline{P}_{t,2}$).



(i) Stage 8 ($P_{t,3}/\overline{P}_{t,2}$).

Figure 6. - Concluded.

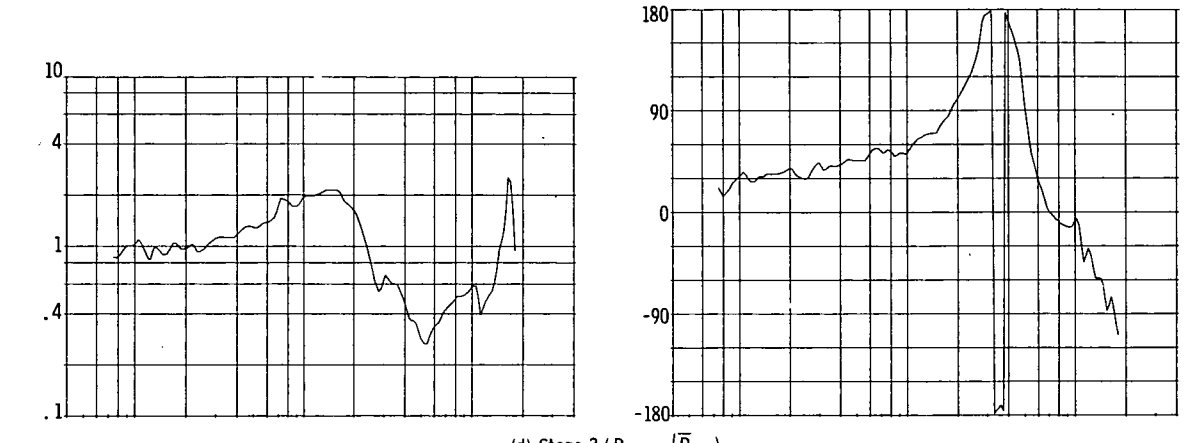


(a) Average compressor-face total pressure ($\bar{P}_{t,2}$/ref.).

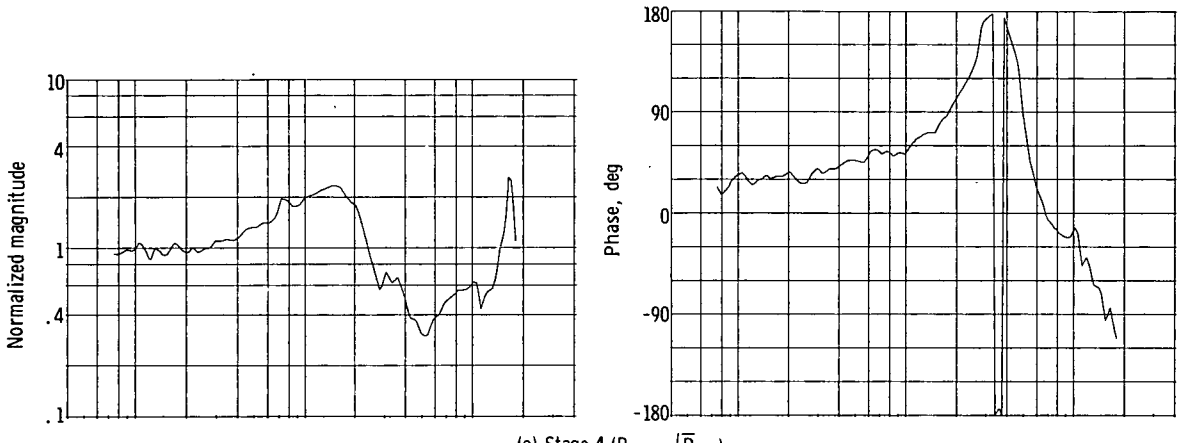
(b) Stage 1 ($P_{t,2.1}/\bar{P}_{t,2}$).

(c) Stage 2 ($P_{t,2.2}/\bar{P}_{t,2}$).

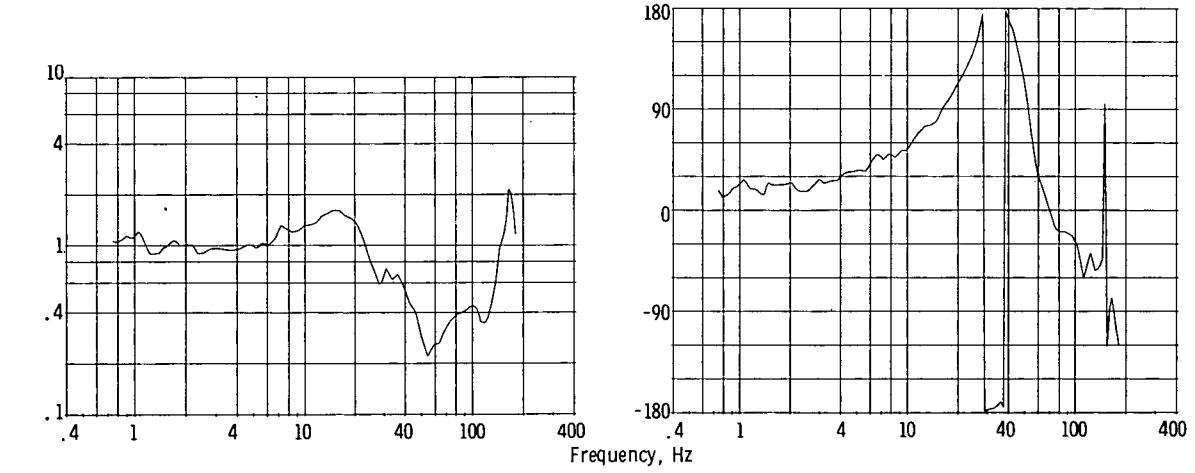
Figure 7. - Normalized frequency responses of engine parameters corresponding to test conditions of 94-percent corrected engine speed, 735-square-centimeter exhaust-nozzle throat area, and untrapped compressor-discharge pressure.



(d) Stage 3 ($P_{t,2.3}/\overline{P}_{t,2}$).

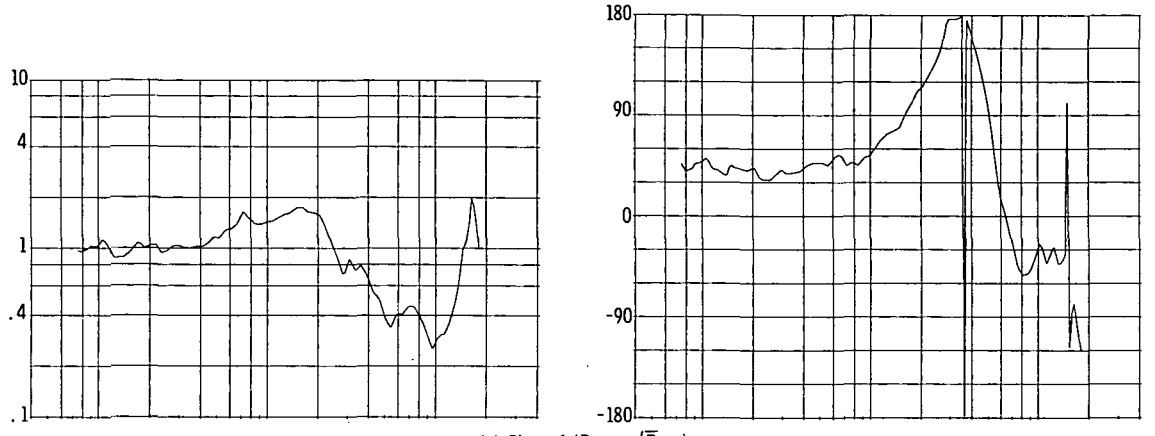


(e) Stage 4 ($P_{t,2.4}/\overline{P}_{t,2}$).

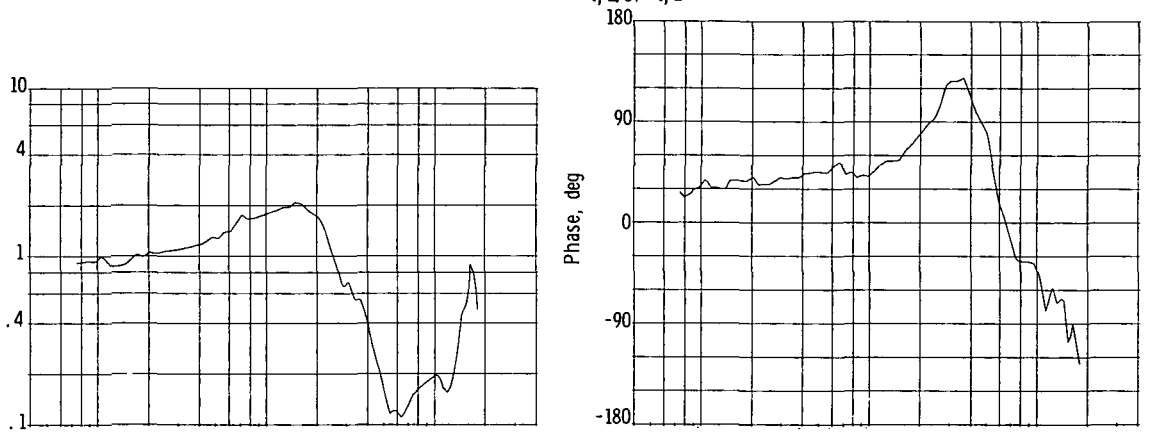


(f) Stage 5 ($P_{t,2.5}/\overline{P}_{t,2}$).

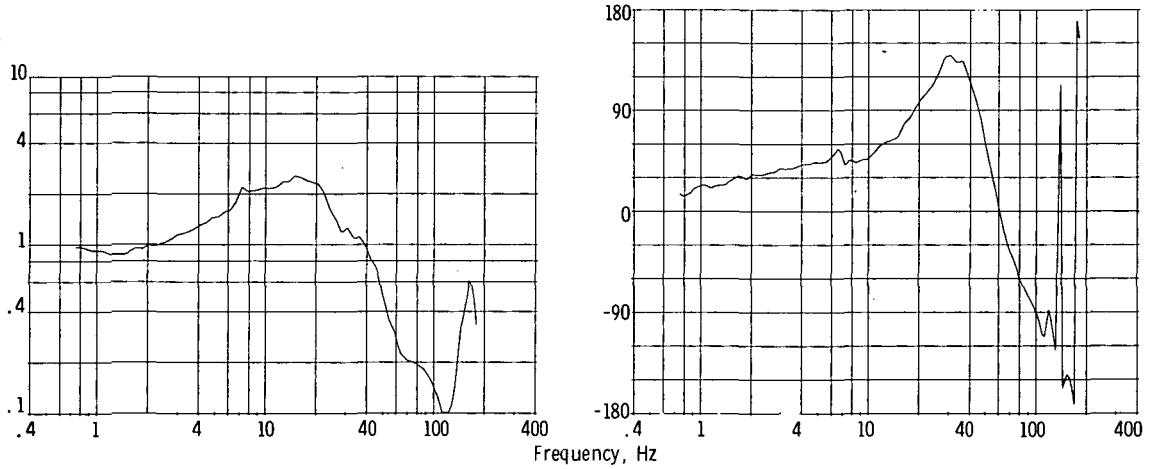
Figure 7. - Continued.



(g) Stage 6 ($P_{t,2.6}/\bar{P}_{t,2}$).

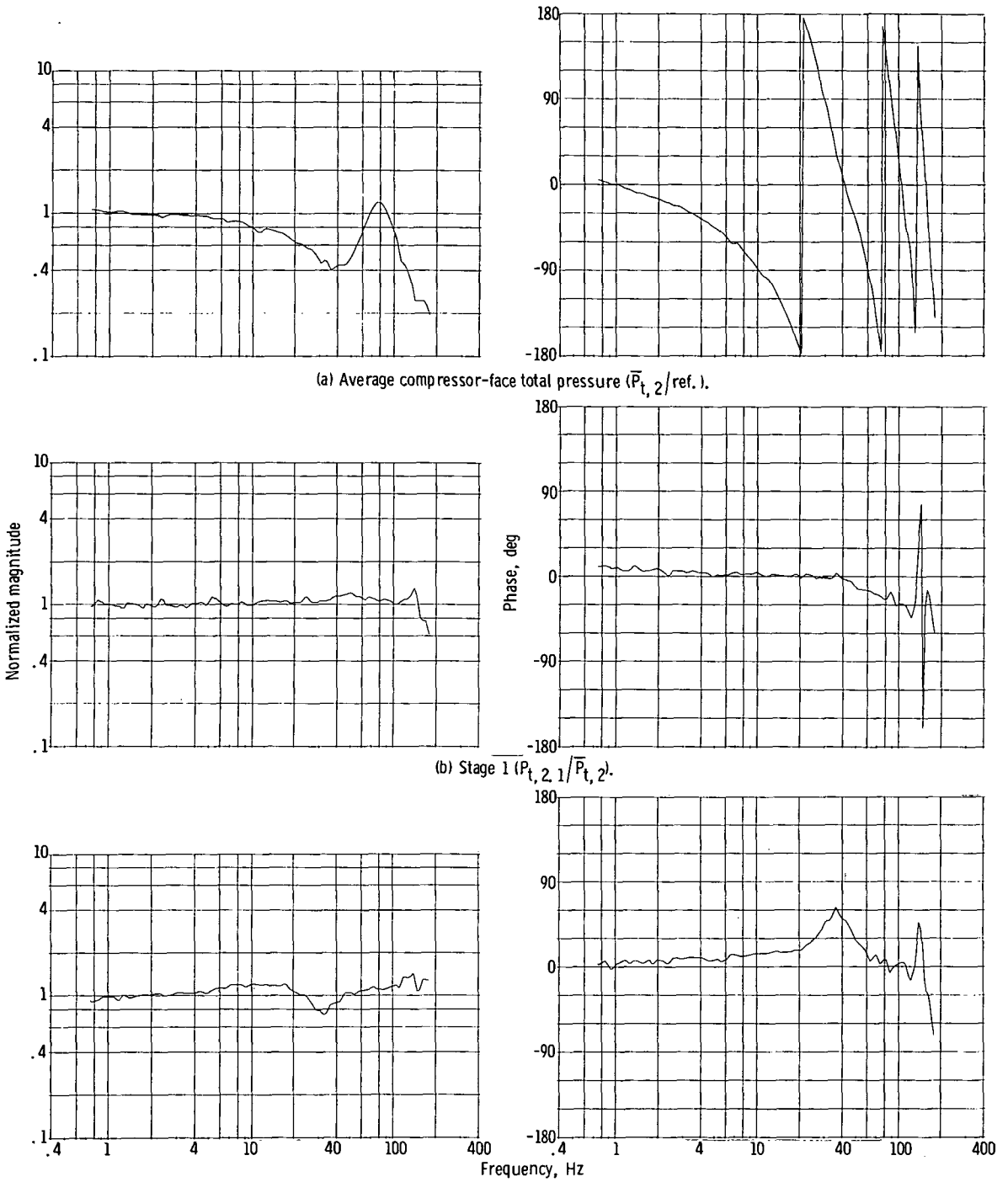


(h) Stage 7 ($P_{t,2.7}/\bar{P}_{t,2}$).



(i) Stage 8 ($P_{t,3}/\bar{P}_{t,2}$).

Figure 7. - Concluded.

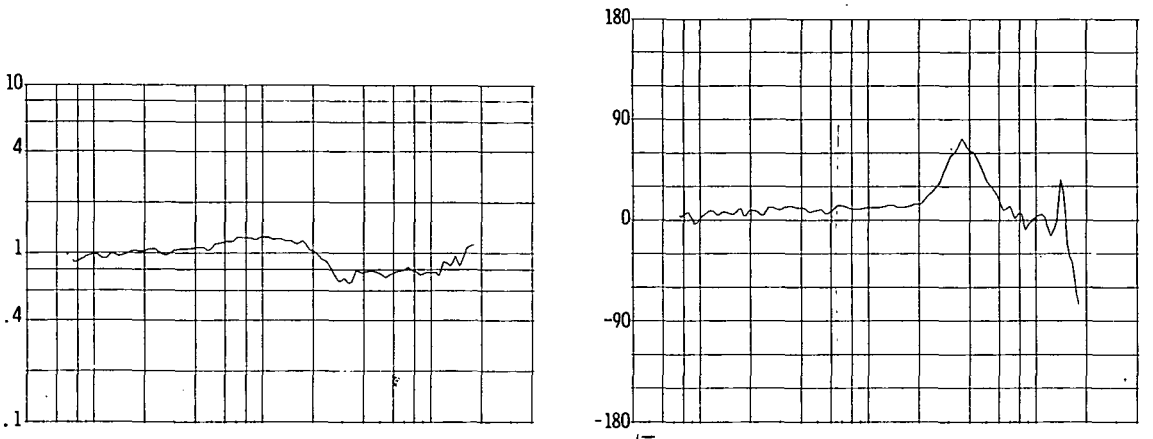


(a) Average compressor-face total pressure ($\overline{P}_{t,2}$/ref.).

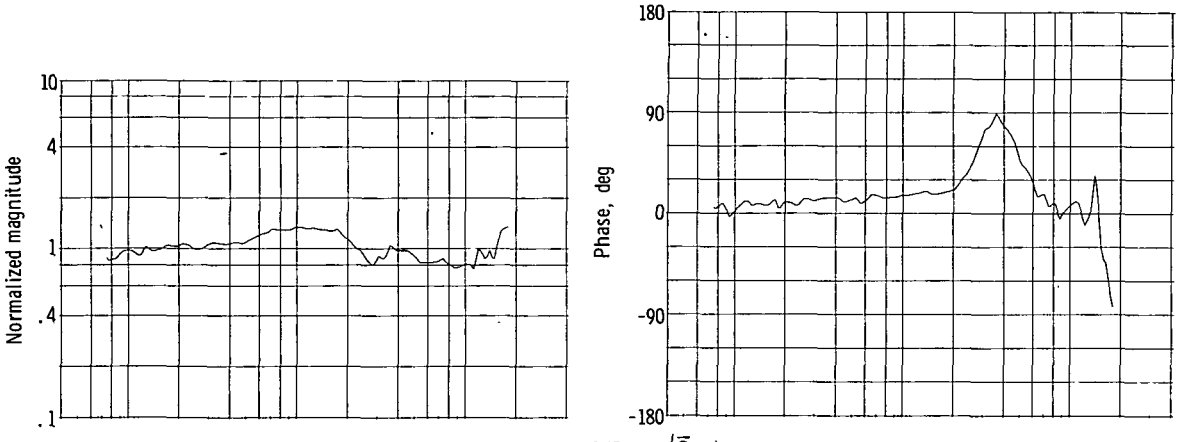
(b) Stage 1 ($P_{t,2.1}/\overline{P}_{t,2}$).

(c) Stage 2 ($P_{t,2.2}/\overline{P}_{t,2}$).

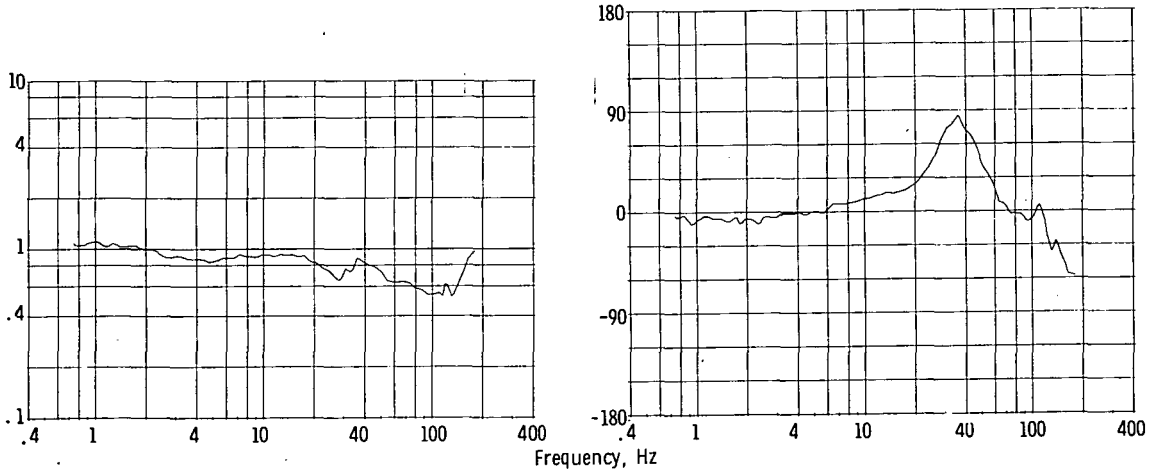
Figure 8. - Normalized frequency responses of engine parameters corresponding to test conditions of 87-percent corrected engine speed, 626-square-centimeter exhaust-nozzle throat area, and trapped compressor-discharge pressure.



(d) Stage 3 ($P_{t,2.3}/\bar{P}_{t,2}$).

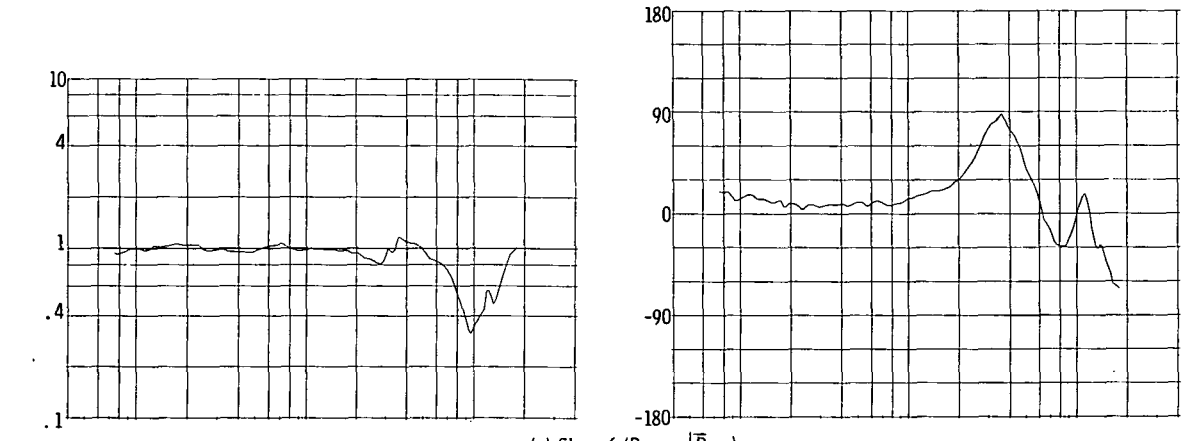


(e) Stage 4 ($P_{t,2.4}/\bar{P}_{t,2}$).

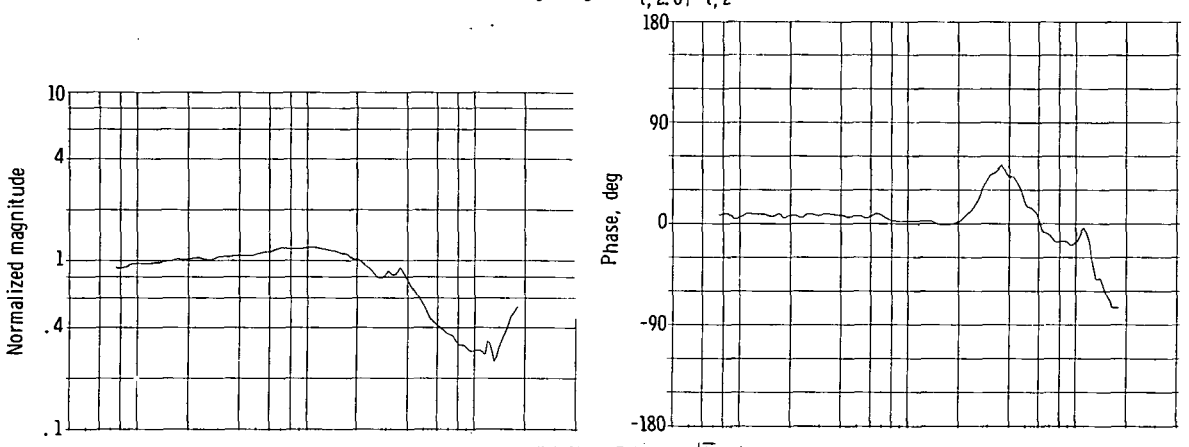


(f) Stage 5 ($P_{t,2.5}/\bar{P}_{t,2}$).

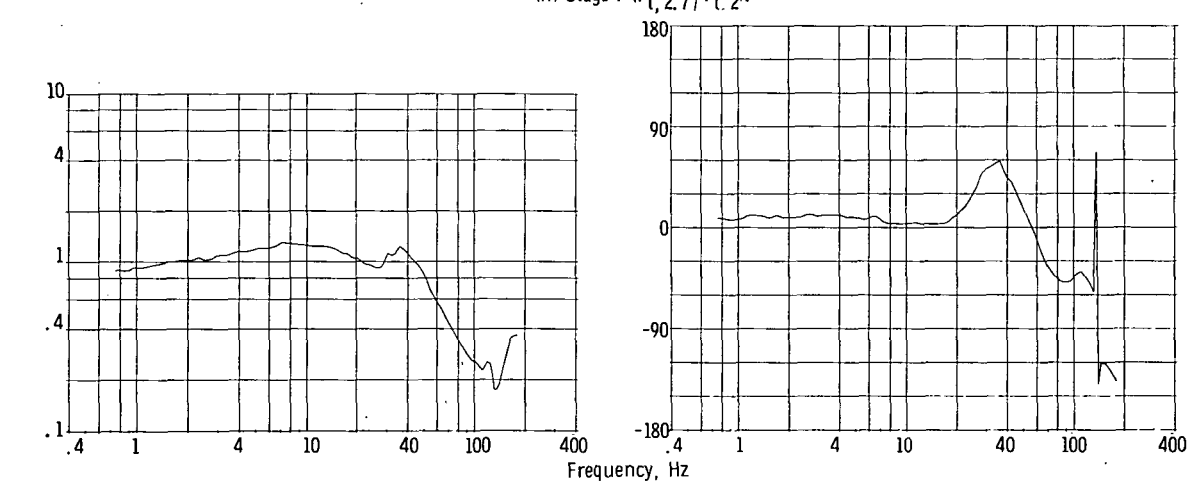
Figure 8. - Continued.



(g) Stage 6 ($P_{t,2.6}/\bar{P}_{t,2}$).

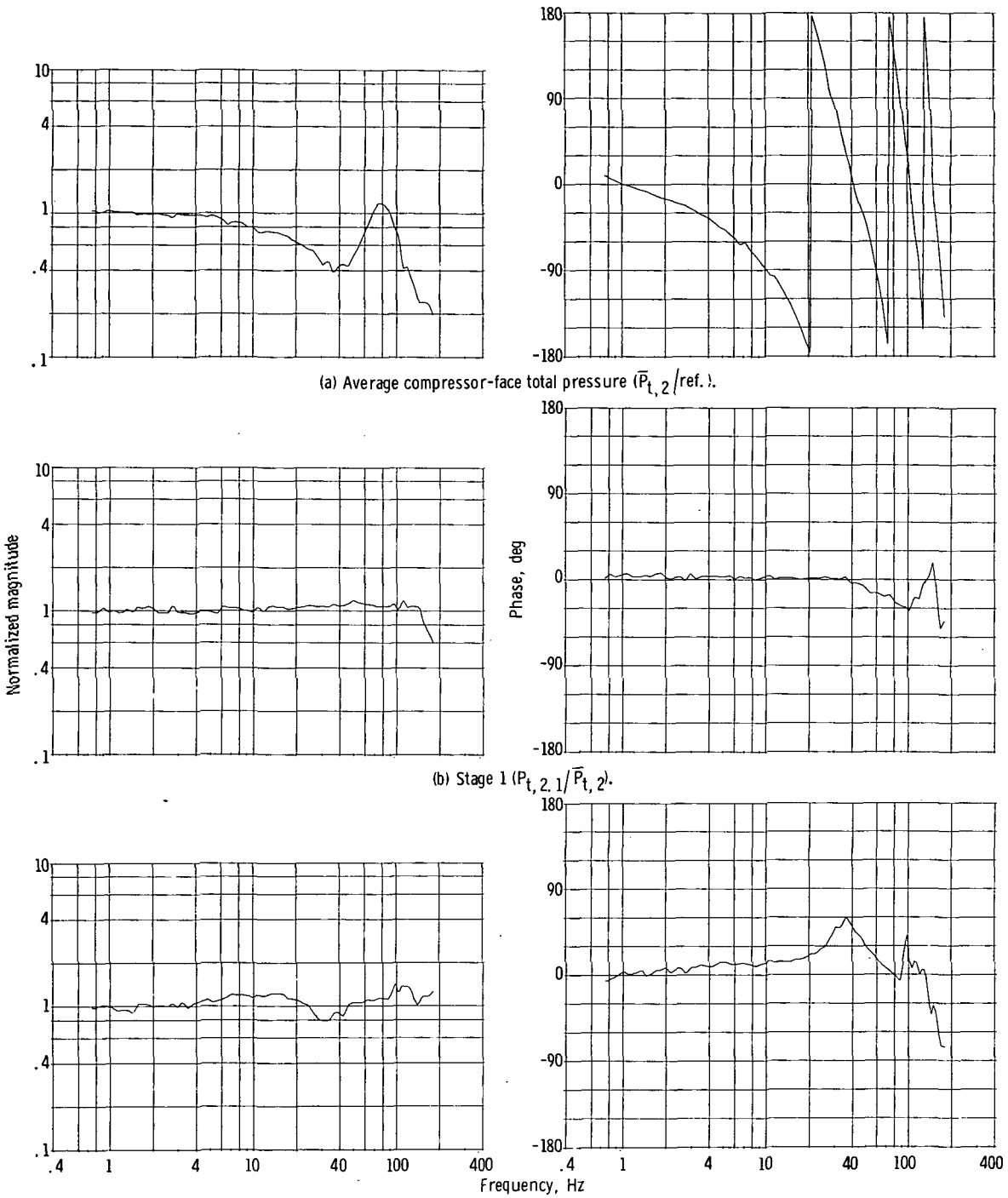


(h) Stage 7 ($P_{t,2.7}/\bar{P}_{t,2}$).



(i) Stage 8 ($P_{t,3}/\bar{P}_{t,2}$).

Figure 8. - Concluded.

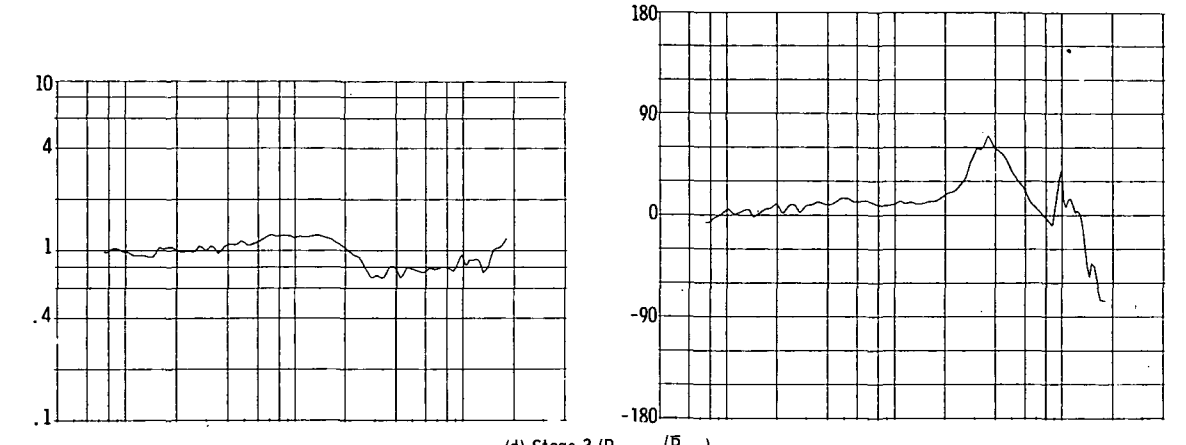


(a) Average compressor-face total pressure ($\bar{P}_{t,2}$/ref.).

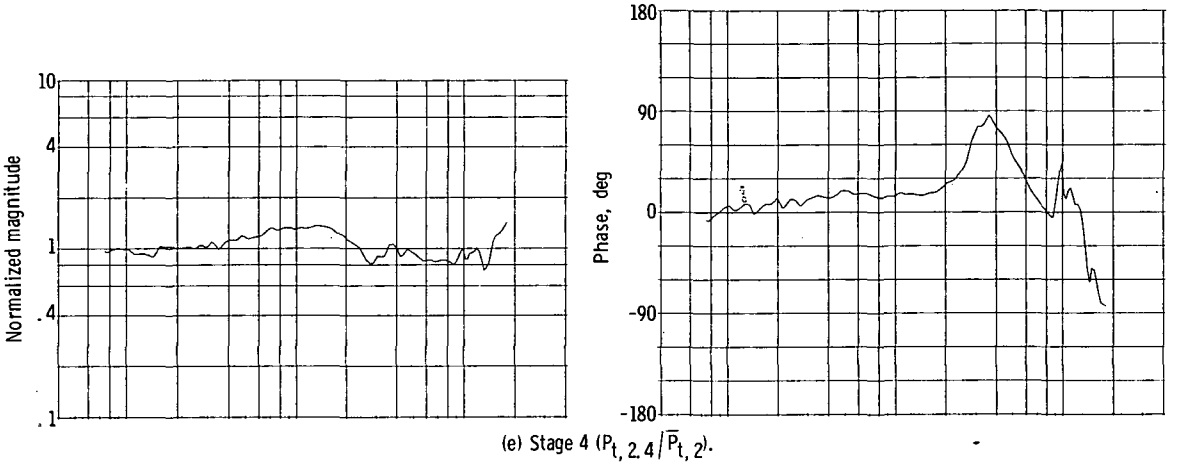
(b) Stage 1 ($P_{t,2.1}/\bar{P}_{t,2}$).

(c) Stage 2 ($P_{t,2.2}/\bar{P}_{t,2}$).

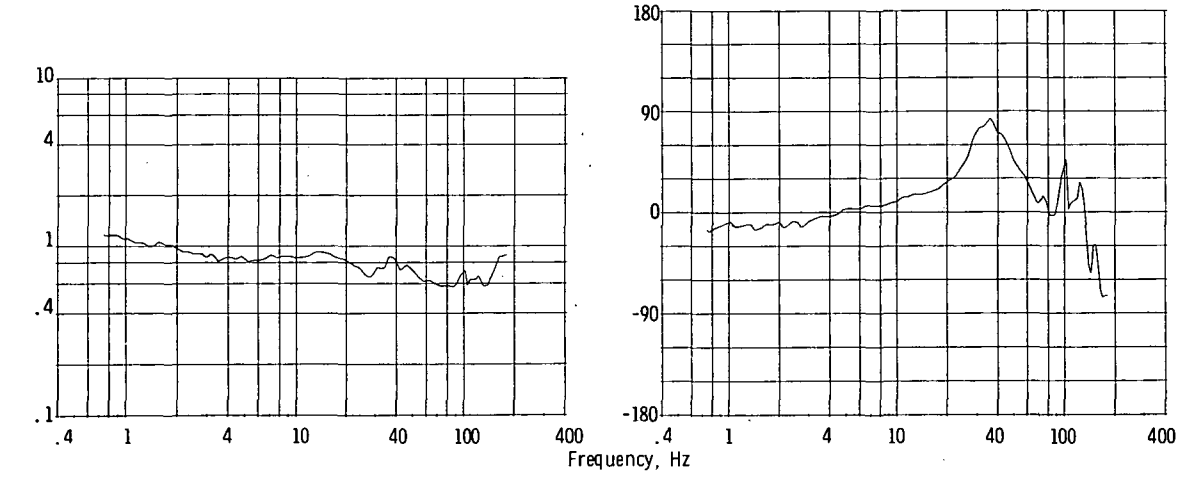
Figure 9. - Normalized frequency responses of engine parameters corresponding to test conditions of 87-percent corrected engine speed, 626-square-centimeter exhaust-nozzle throat area, and untrapped compressor-discharge pressure.



(d) Stage 3 ($P_{t,2.3}/\bar{P}_{t,2}$).

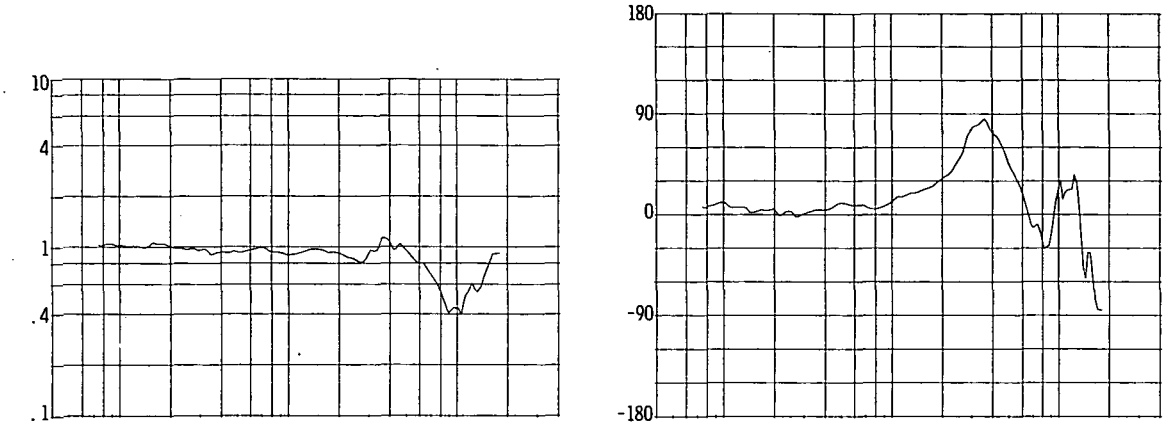


(e) Stage 4 ($P_{t,2.4}/\bar{P}_{t,2}$).

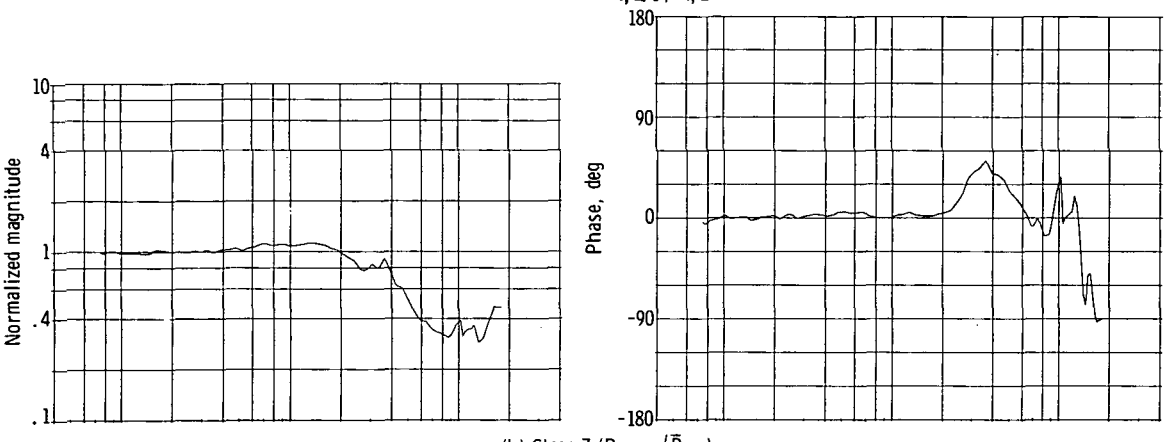


(f) Stage 5 ($P_{t,2.5}/\bar{P}_{t,2}$).

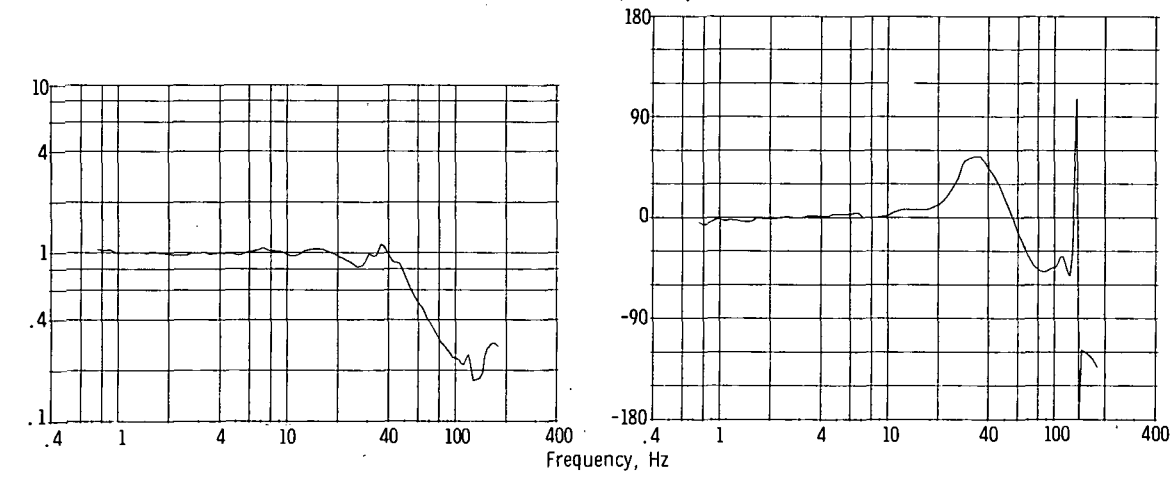
Figure 9. - Continued.



(g) Stage 6 ($P_{t,2.6}/\bar{P}_{t,2}$).

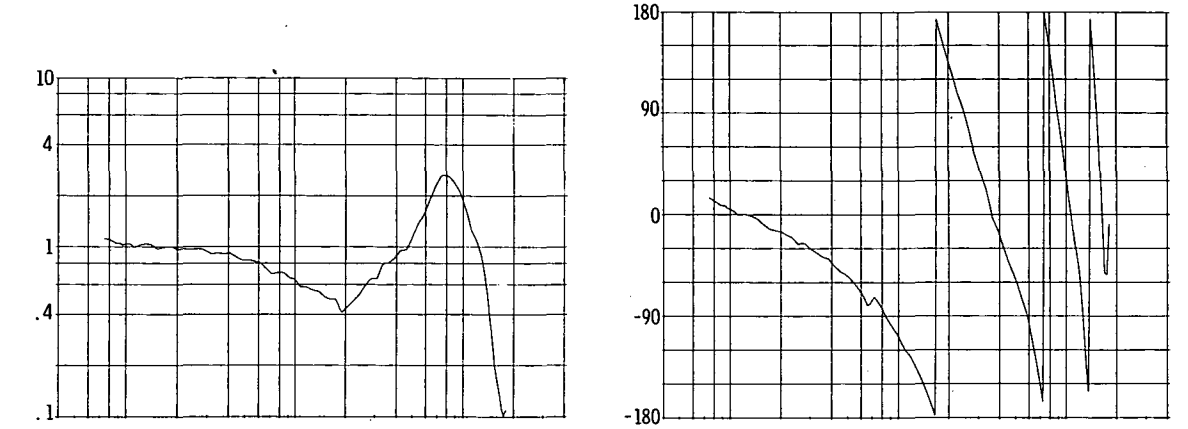


(h) Stage 7 ($P_{t,2.7}/\bar{P}_{t,2}$).

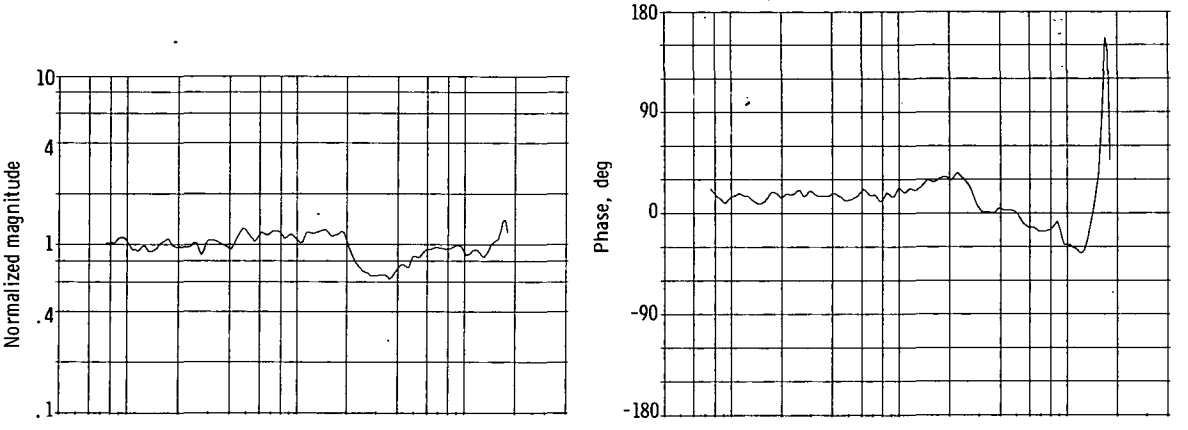


(i) Stage 8 ($P_{t,3}/\bar{P}_{t,2}$).

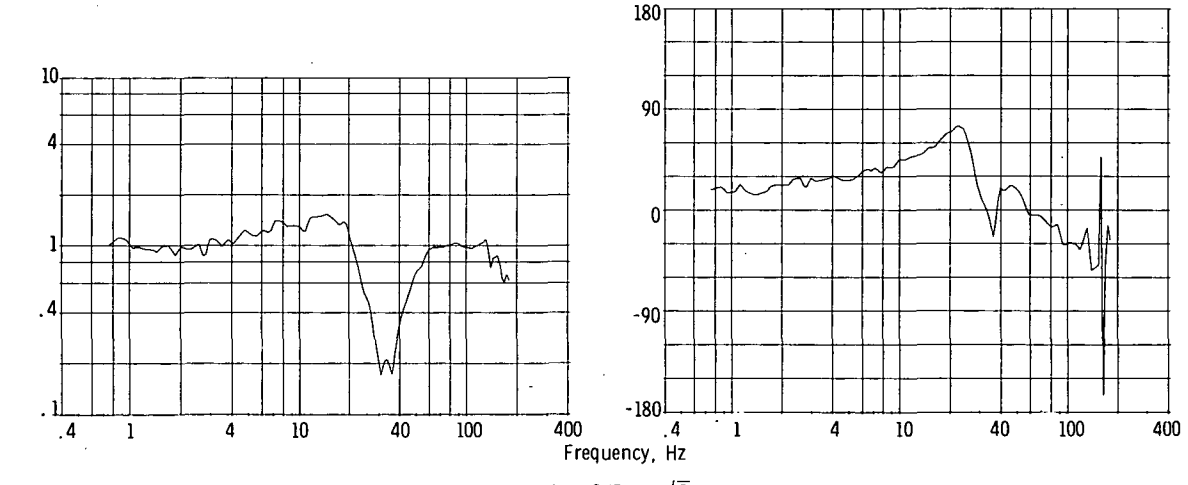
Figure 9. - Concluded.



(a) Average compressor-face total pressure ($\overline{P}_{t,2}$/ref.).

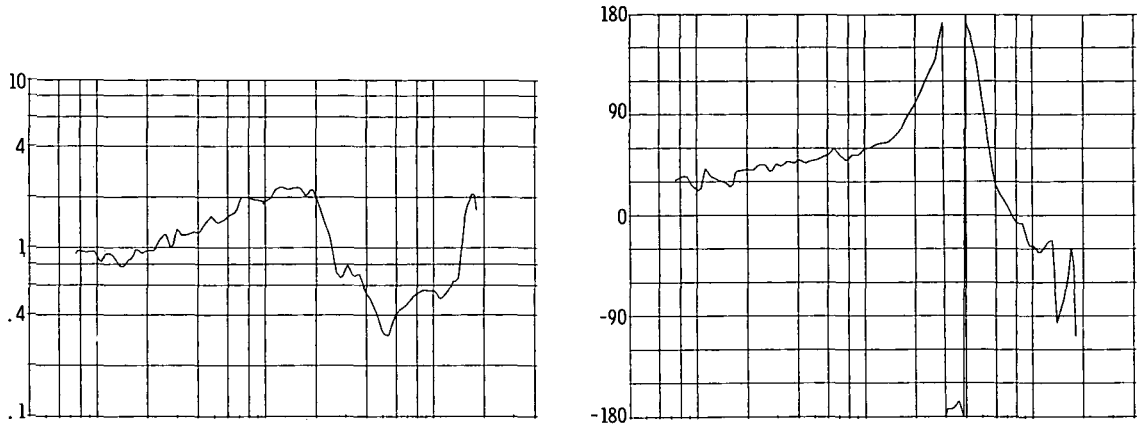


(b) Stage 1 ($P_{t,2.1}/\overline{P}_{t,2}$).

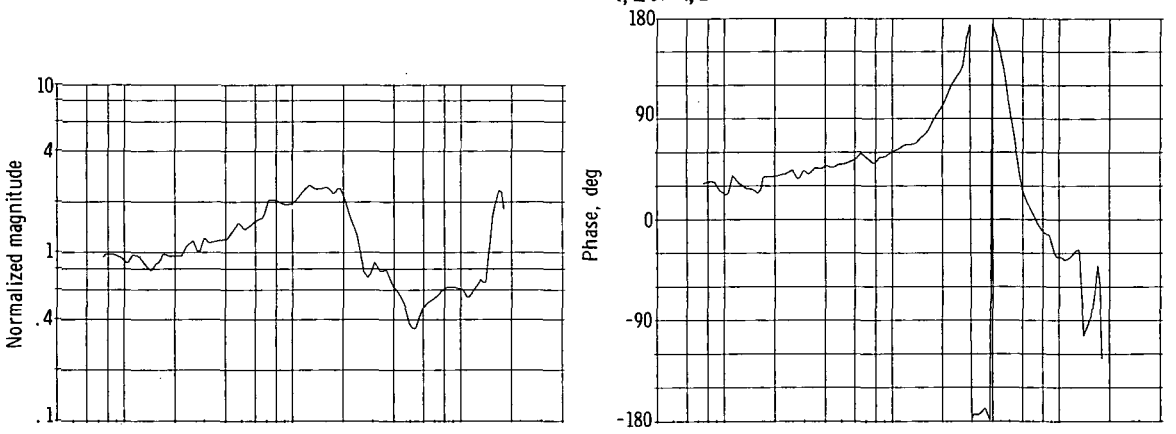


(c) Stage 2 ($P_{t,2.2}/\overline{P}_{t,2}$).

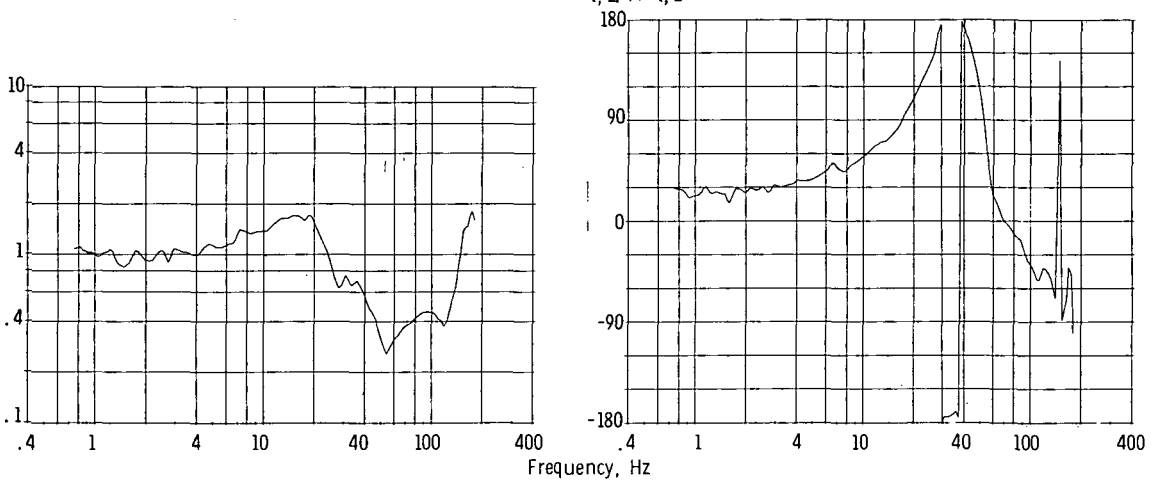
Figure 10. - Normalized frequency responses of engine parameters corresponding to test conditions of 94-percent corrected engine speed, 677-square-centimeter exhaust-nozzle throat area, and trapped compressor-discharge pressure.



(d) Stage 3 ($P_{t,2.3}/\overline{P}_{t,2}$).

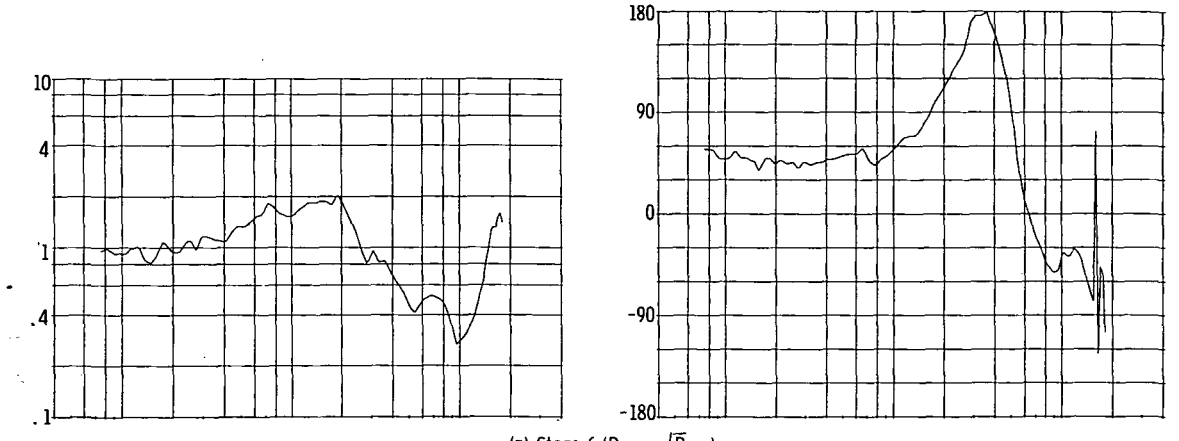


(e) Stage 4 ($P_{t,2.4}/\overline{P}_{t,2}$).

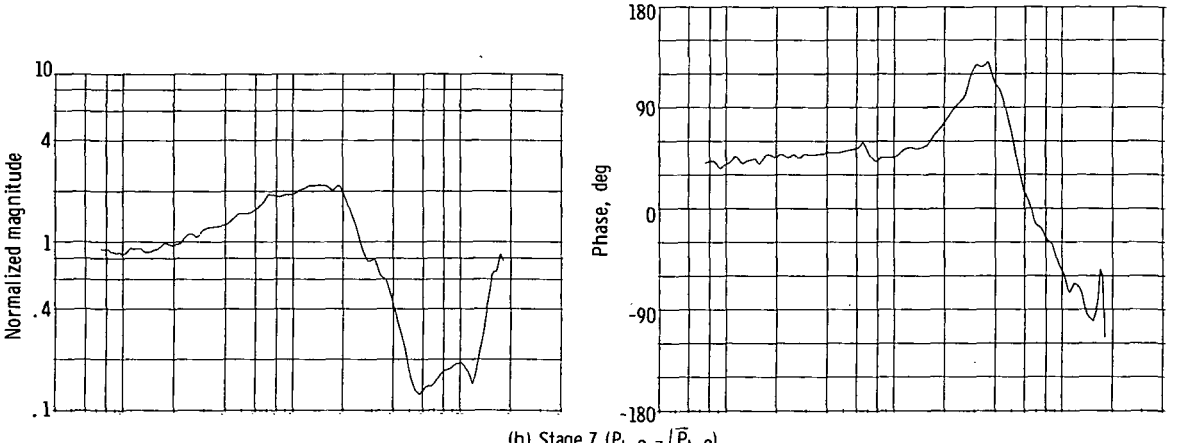


(f) Stage 5 ($P_{t,2.5}/\overline{P}_{t,2}$).

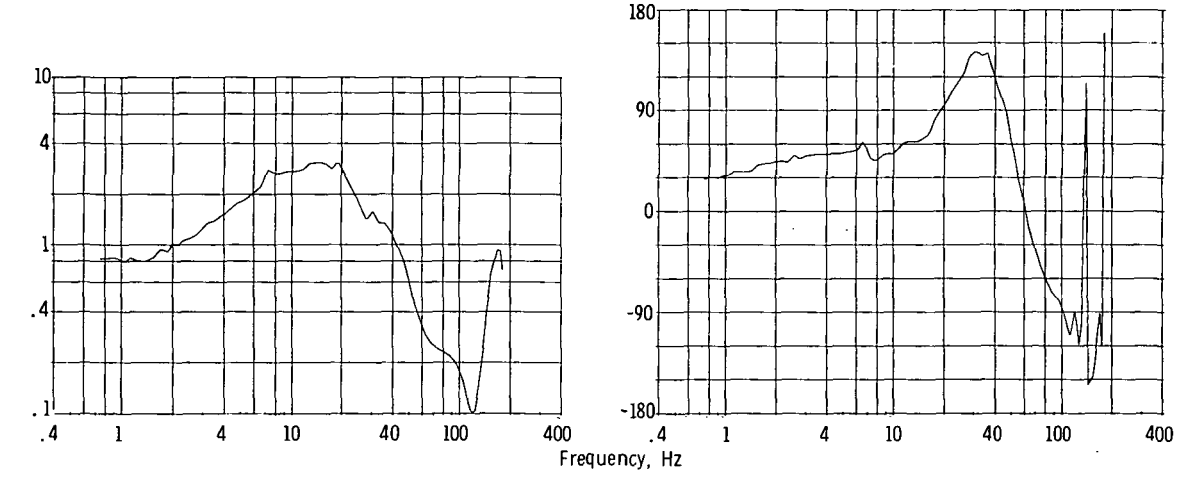
Figure 10. - Continued.



(g) Stage 6 ($P_{t,2.6}/\overline{P}_{t,2}$).

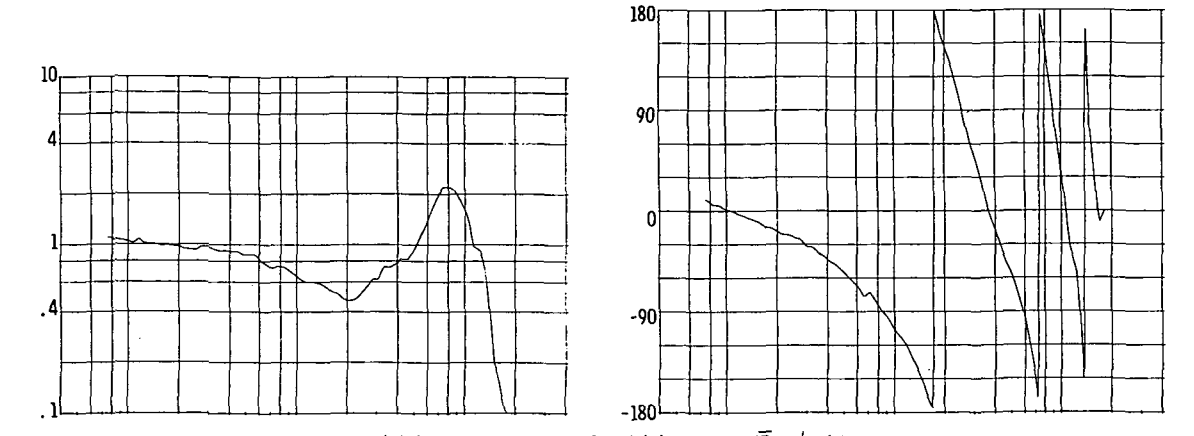


(h) Stage 7 ($P_{t,2.7}/\overline{P}_{t,2}$).

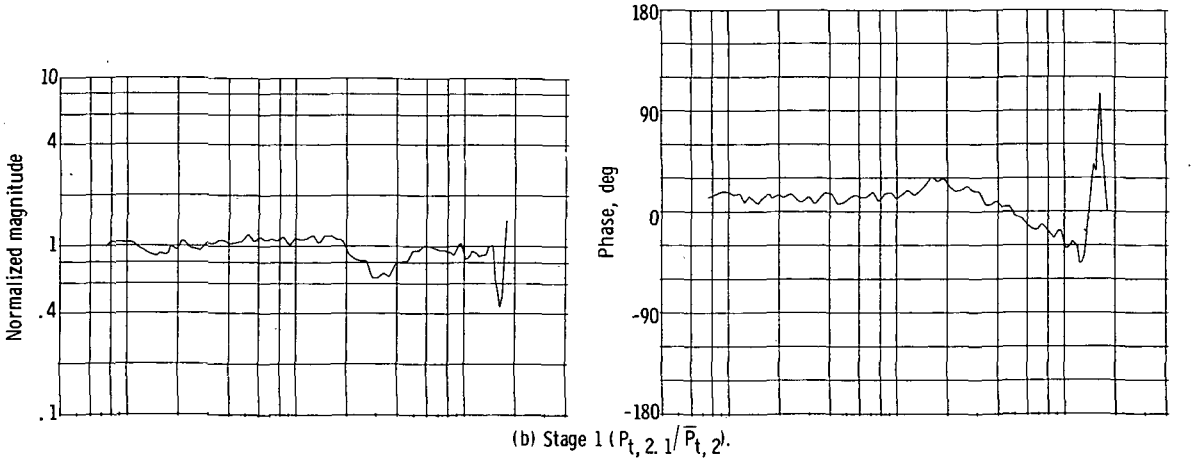


(i) Stage 8 ($P_{t,3}/\overline{P}_{t,2}$).

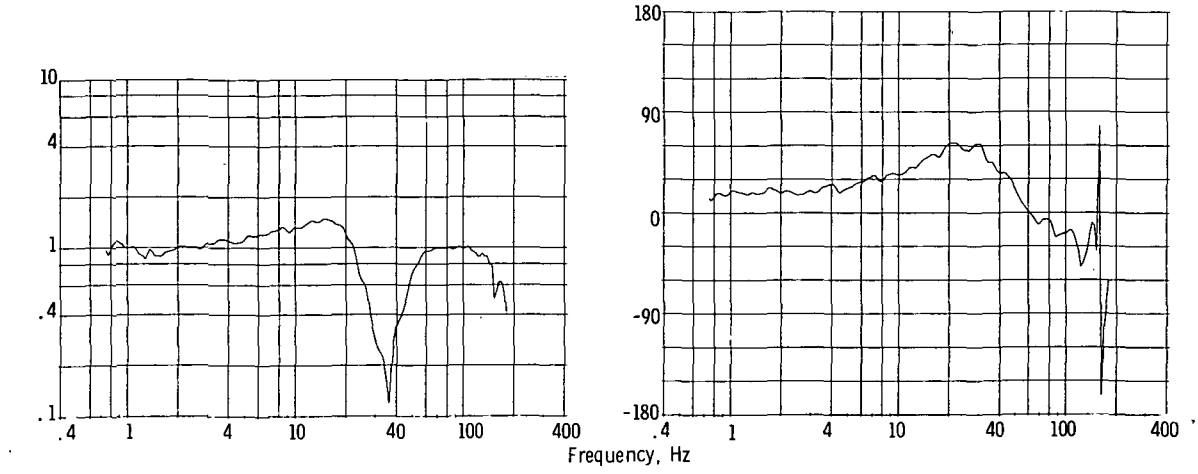
Figure 10. - Concluded.



(a) Average compressor-face total pressure ($\bar{P}_{t,2}$/ref.).

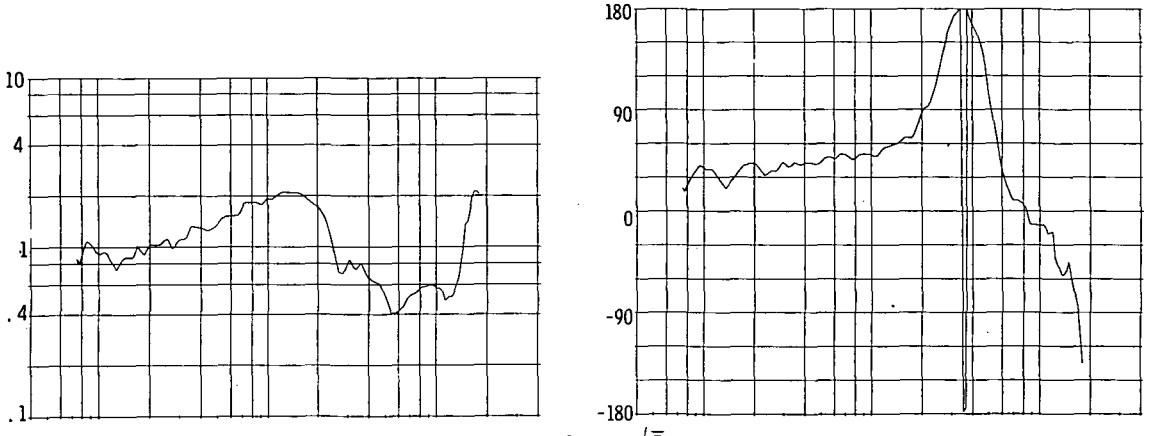


(b) Stage 1 ($P_{t,2.1}/\bar{P}_{t,2}$).

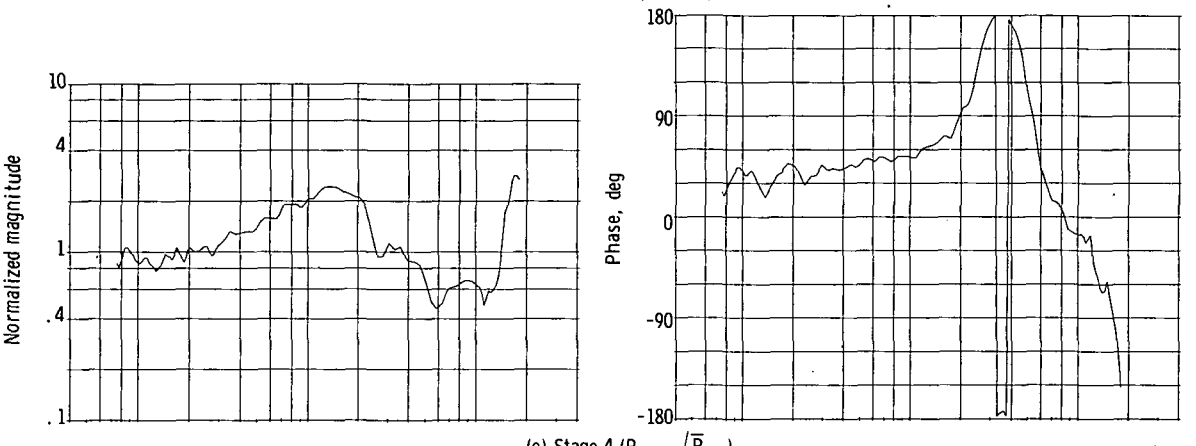


(c) Stage 2 ($P_{t,2.2}/\bar{P}_{t,2}$).

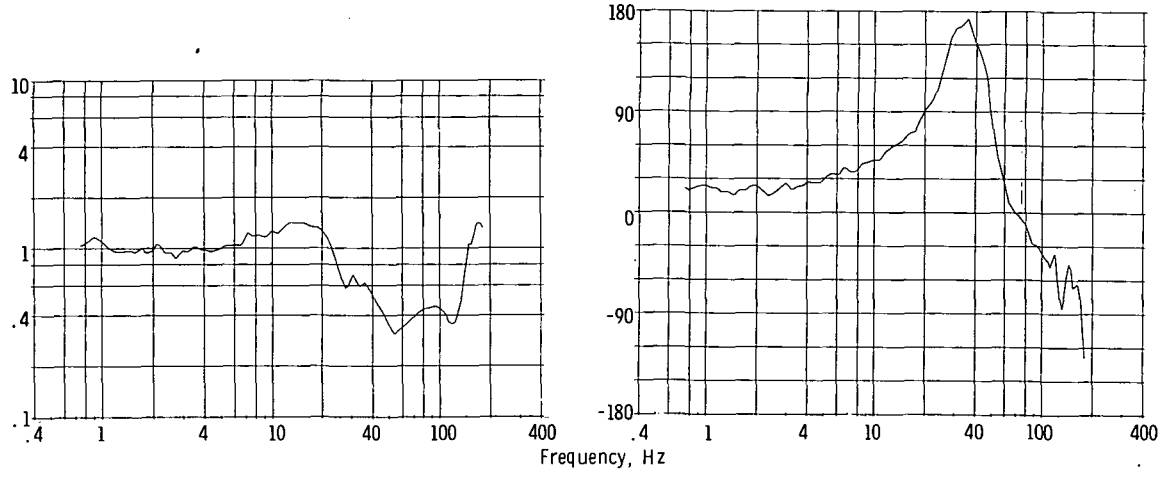
Figure 11. - Normalized frequency responses of engine parameters corresponding to test conditions of 94-percent corrected engine speed, 626-square-centimeter exhaust-nozzle throat area, and trapped compressor-discharge pressure.



(d) Stage 3 ($P_{t,2.3}/\bar{P}_{t,2}$).

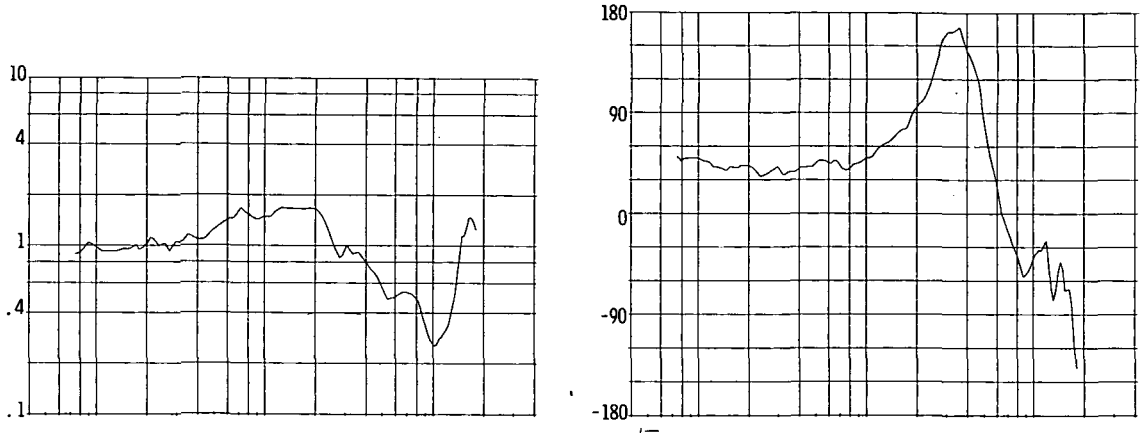


(e) Stage 4 ($P_{t,2.4}/\bar{P}_{t,2}$).

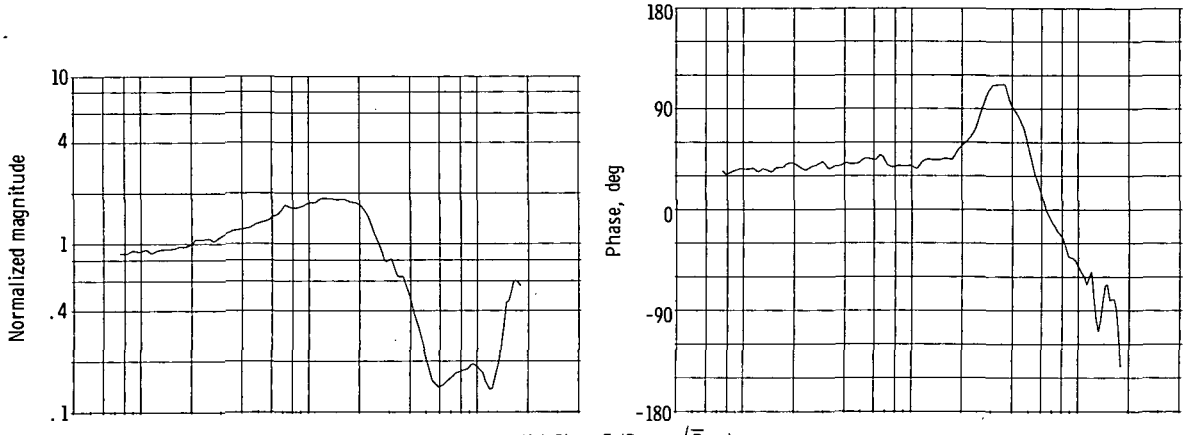


(f) Stage 5 ($P_{t,2.5}/\bar{P}_{t,2}$).

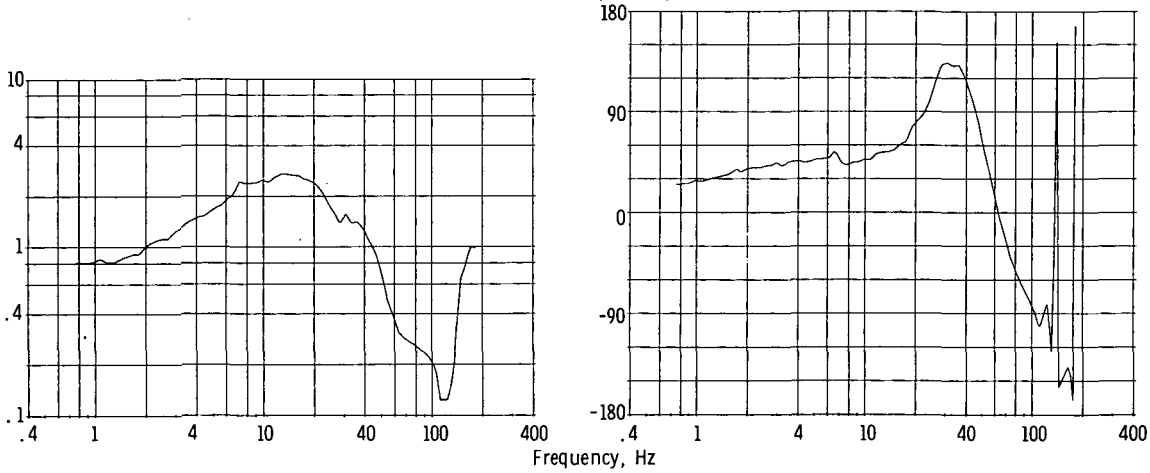
Figure 11. - Continued.



(g) Stage 6 ($P_{t,2.6}/\overline{P}_{t,2}$).

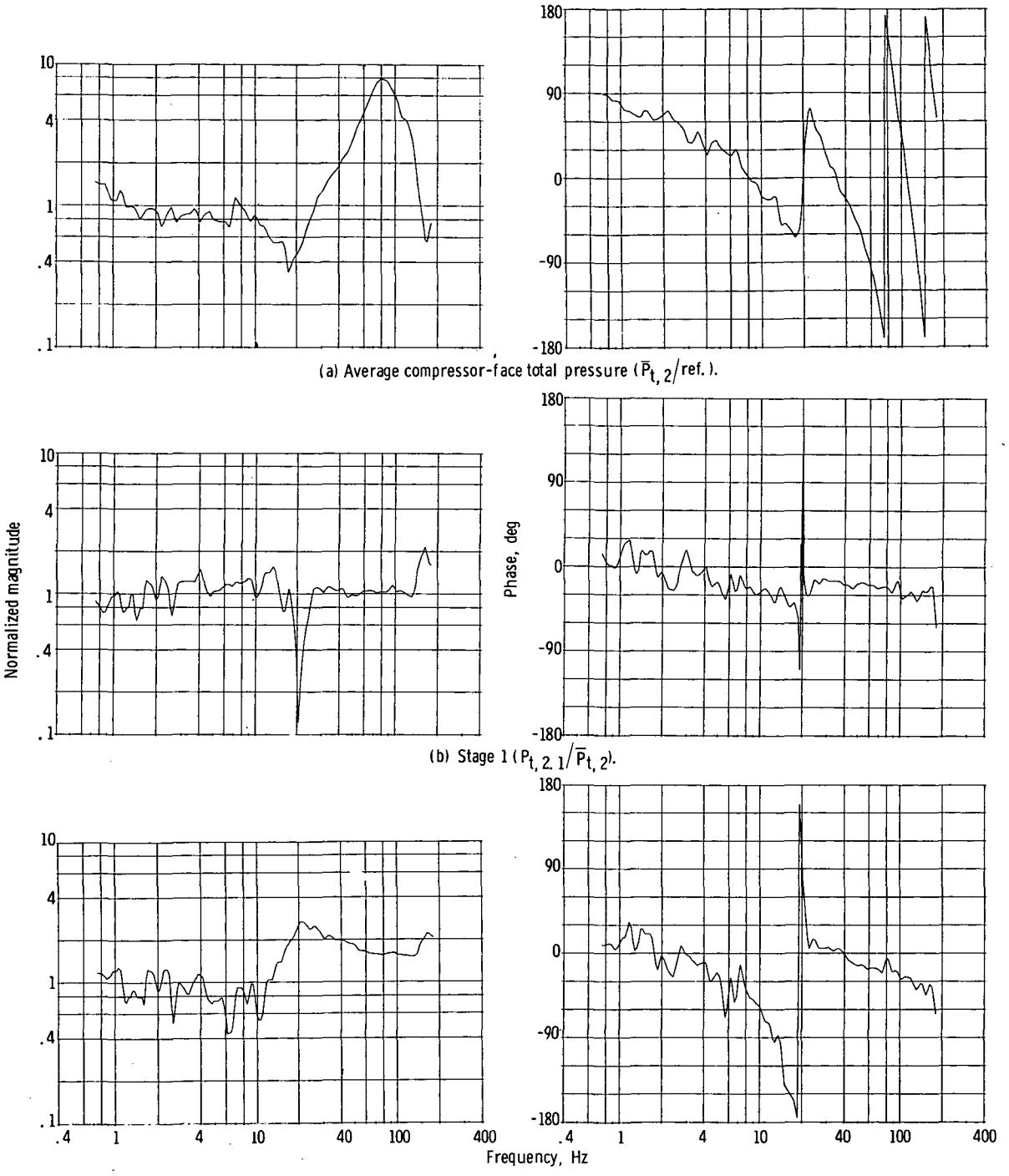


(h) Stage 7 ($P_{t,2.7}/\overline{P}_{t,2}$).



(i) Stage 8 ($P_{t,3}/\overline{P}_{t,2}$).

Figure 11. Concluded.

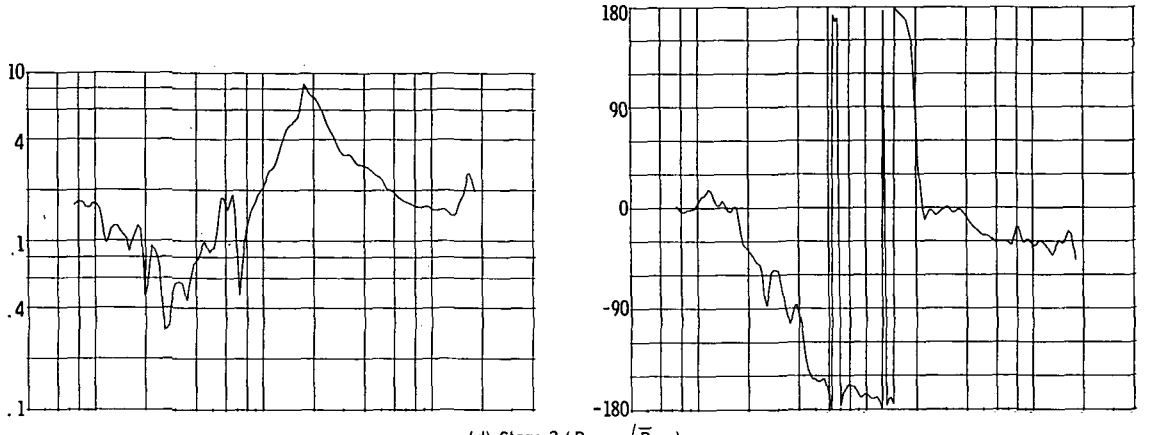


(a) Average compressor-face total pressure ($\bar{P}_{t,2}$/ref.).

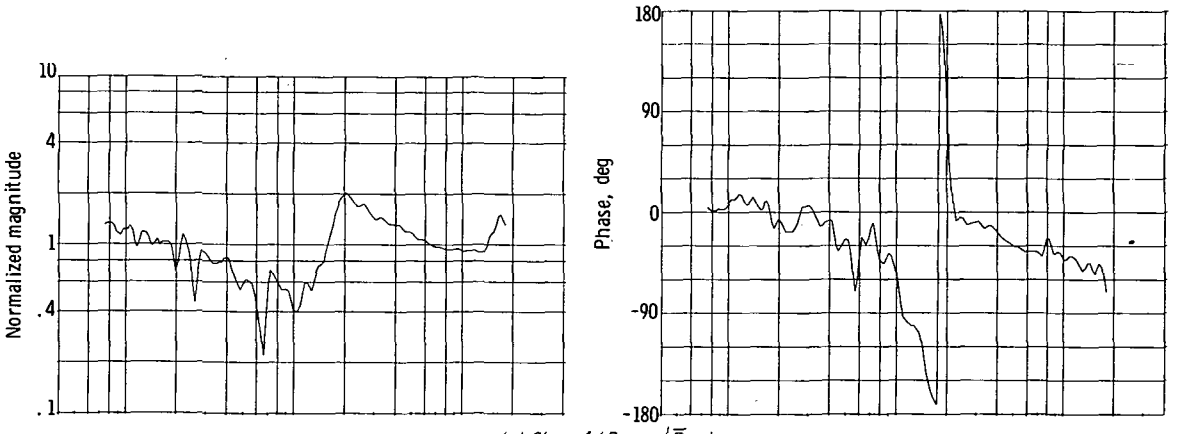
(b) Stage 1 ($P_{t,2.1}/\bar{P}_{t,2}$).

(c) Stage 2 ($P_{t,2.2}/\bar{P}_{t,2}$).

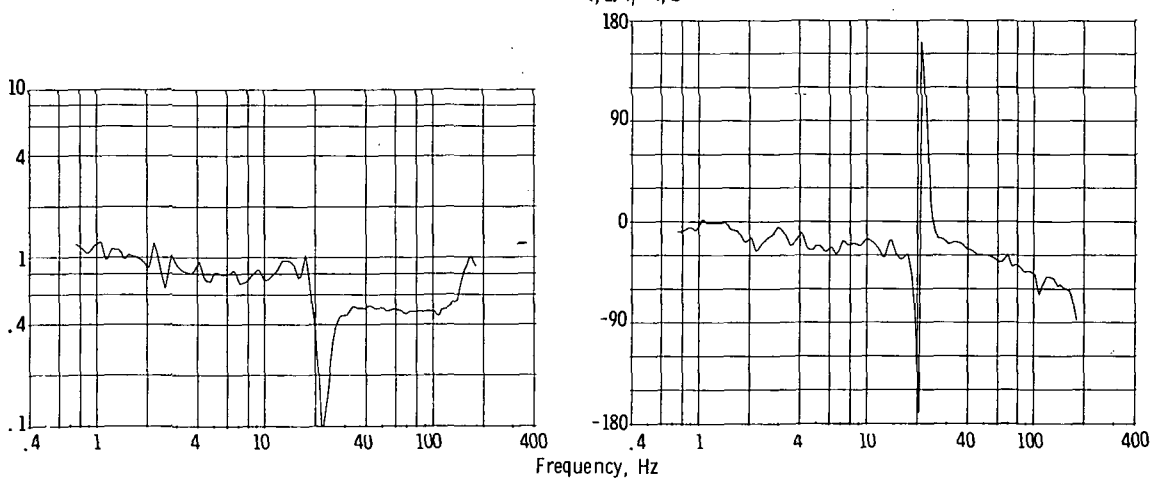
Figure 12. - Normalized frequency responses of engine parameters corresponding to test conditions of 100-percent corrected engine speed, 735-square-centimeter exhaust-nozzle throat area, and untrapped compressor-discharge pressure.



(d) Stage 3 ($P_{t,2.3}/\overline{P}_{t,2}$).

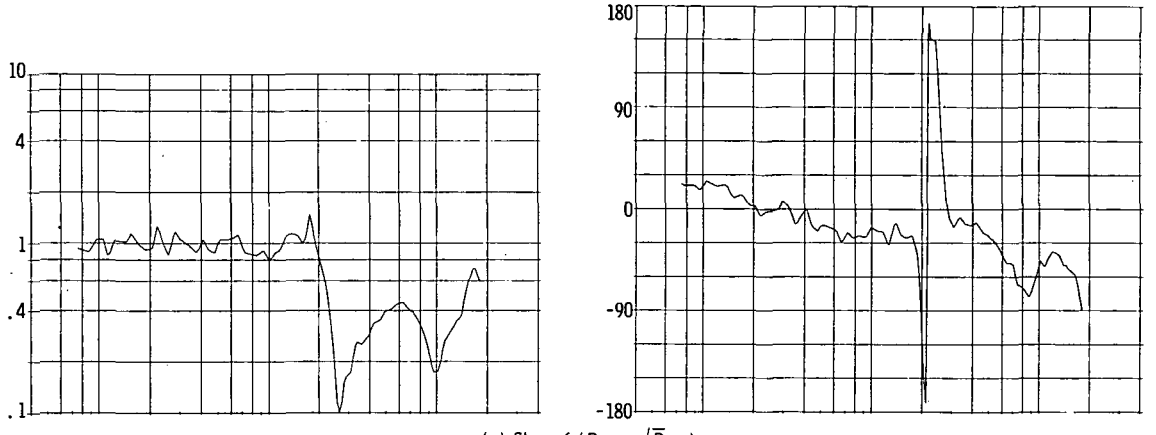


(e) Stage 4 ($P_{t,2.4}/\overline{P}_{t,2}$).

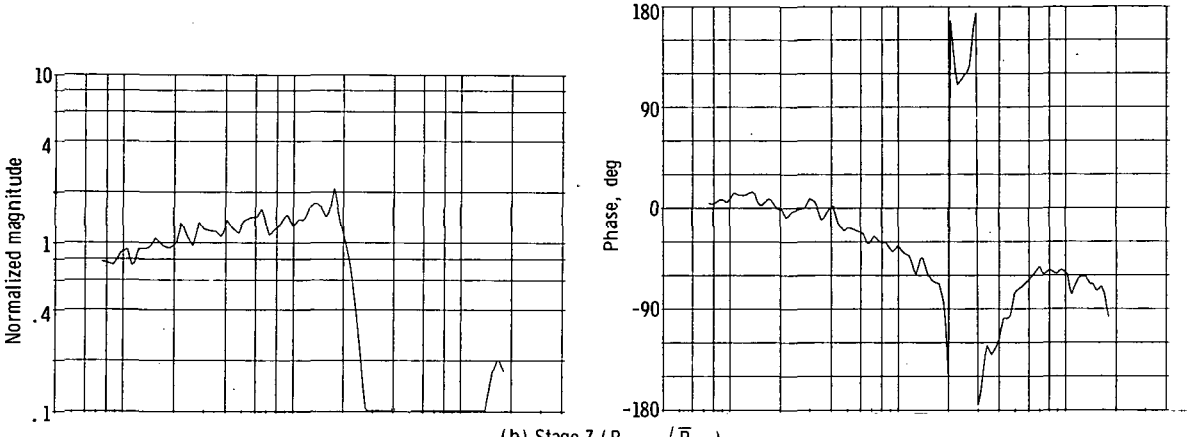


(f) Stage 5 ($P_{t,2.5}/\overline{P}_{t,2}$).

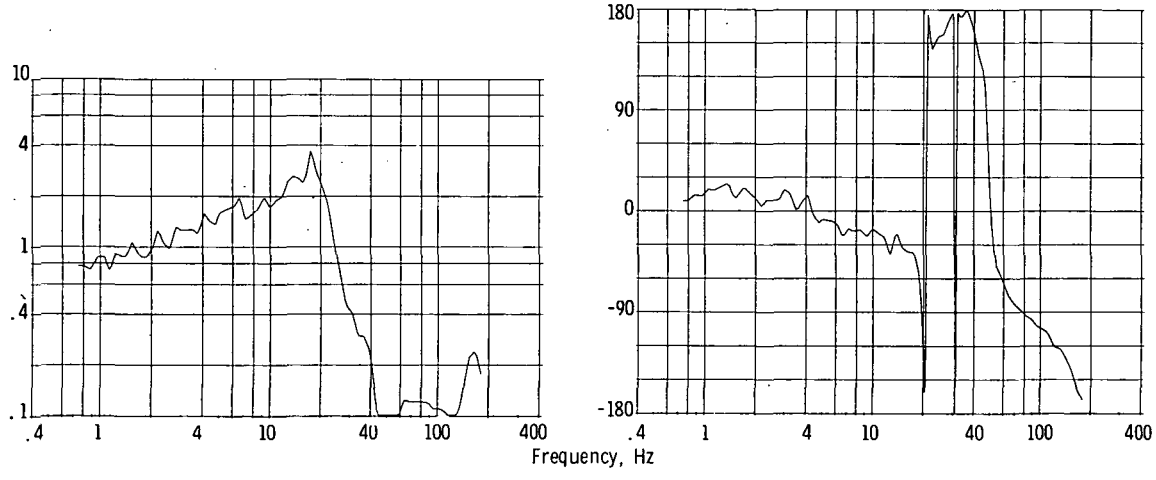
Figure 12. - Continued.



(g) Stage 6 ($P_{t,2.6}/\overline{P}_{t,2}$).

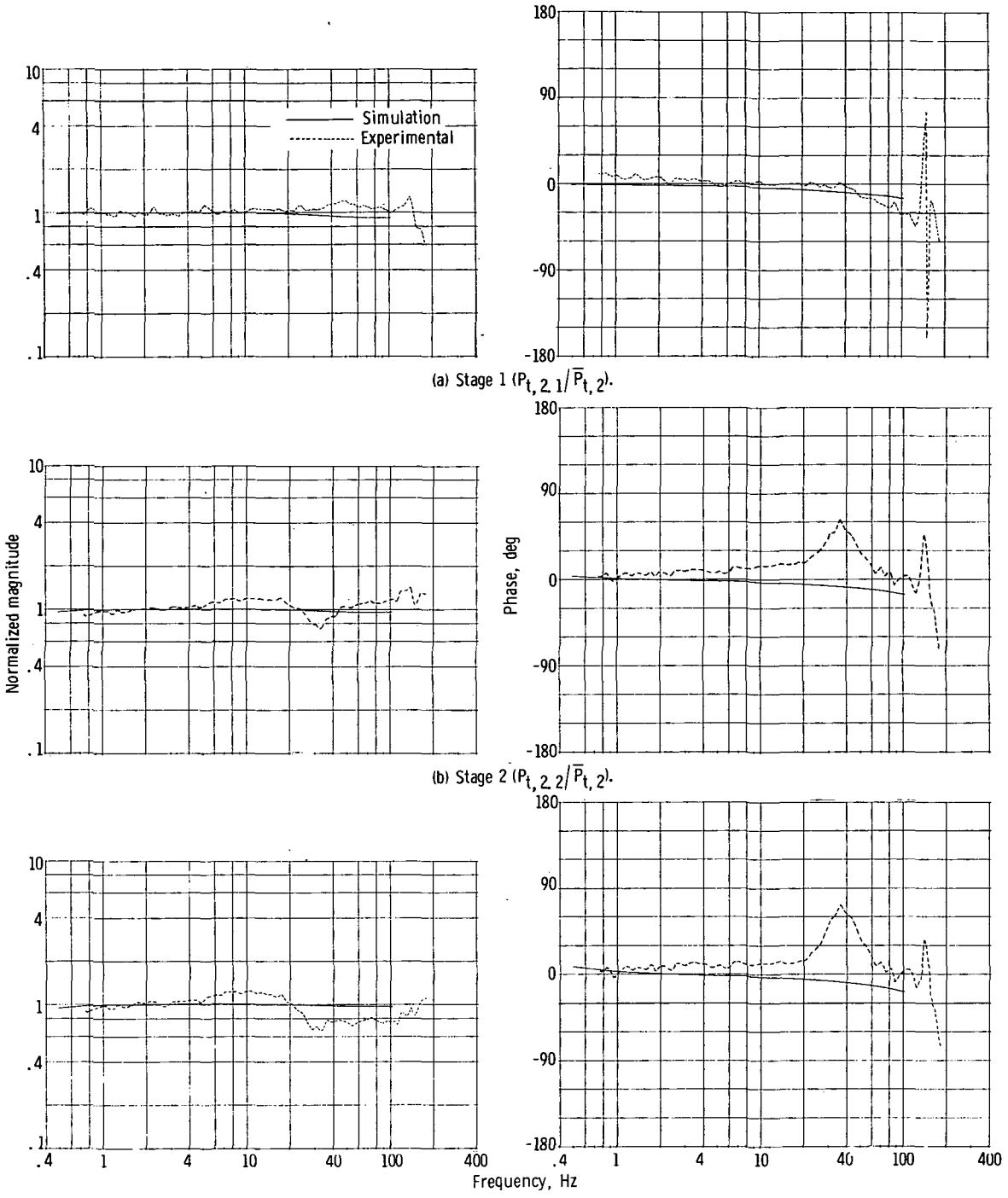


(h) Stage 7 ($P_{t,2.7}/\overline{P}_{t,2}$).



(i) Stage 8 ($P_{t,3}/\overline{P}_{t,2}$).

Figure 12. - Concluded.

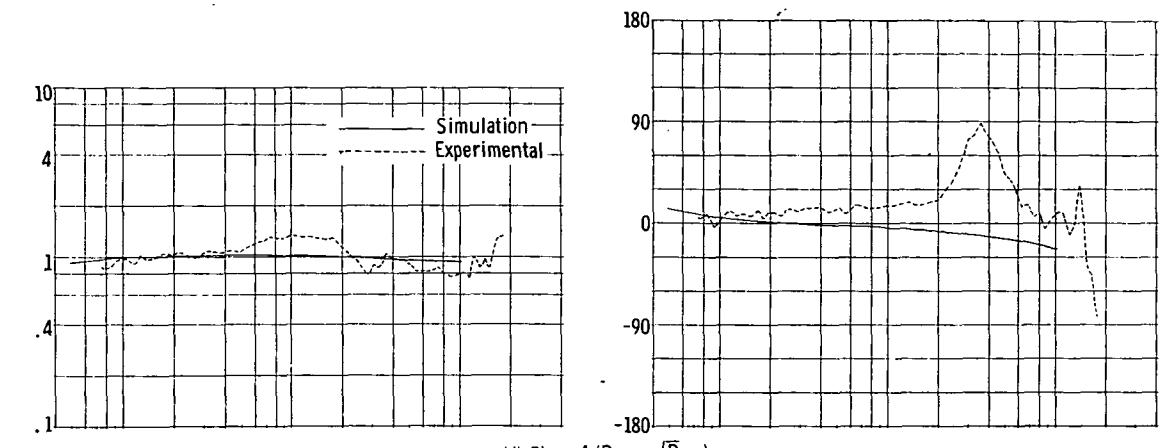


(a) Stage 1 ($P_{t,2.1}/\bar{P}_{t,2}$).

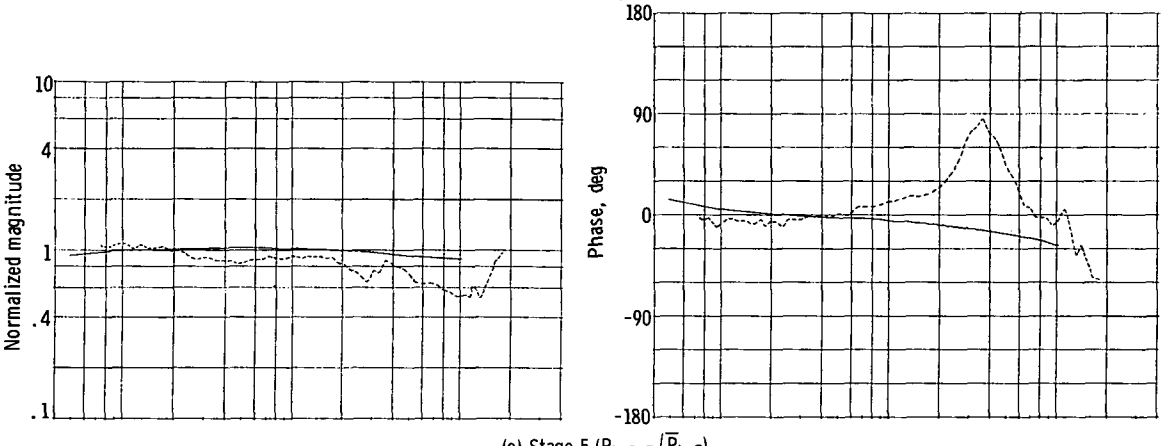
(b) Stage 2 ($P_{t,2.2}/\bar{P}_{t,2}$).

(c) Stage 3 ($P_{t,2.3}/\bar{P}_{t,2}$).

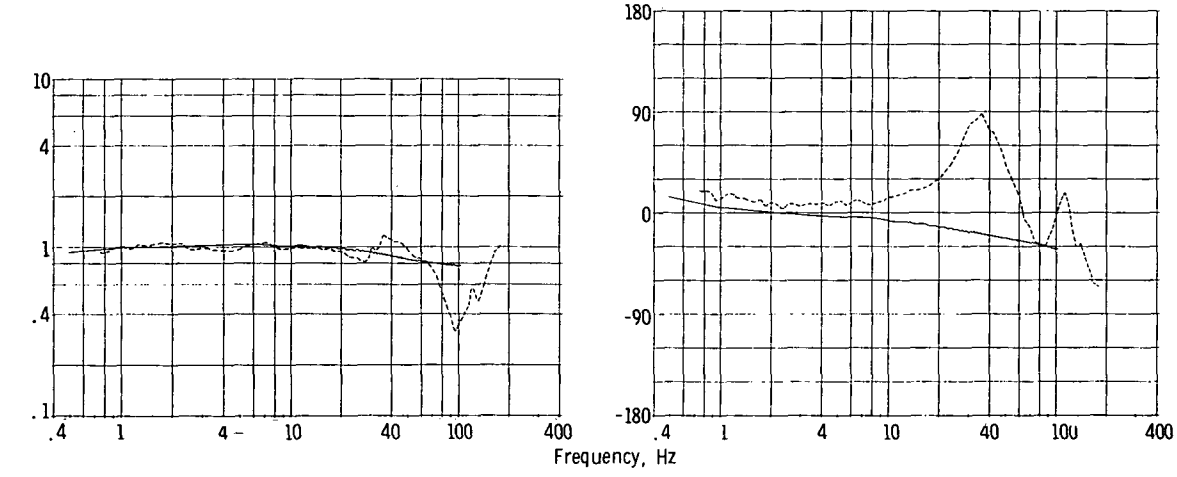
Figure 13. - Comparison of normalized frequency responses of engine parameters from simulation (ref. 6) and from actual engine for test conditions of 87-percent corrected engine speed, 626-square-centimeter exhaust-nozzle throat area, and trapped compressor-discharge pressure.



(d) Stage 4 ($P_{t,2.4}/\bar{P}_{t,2}$).

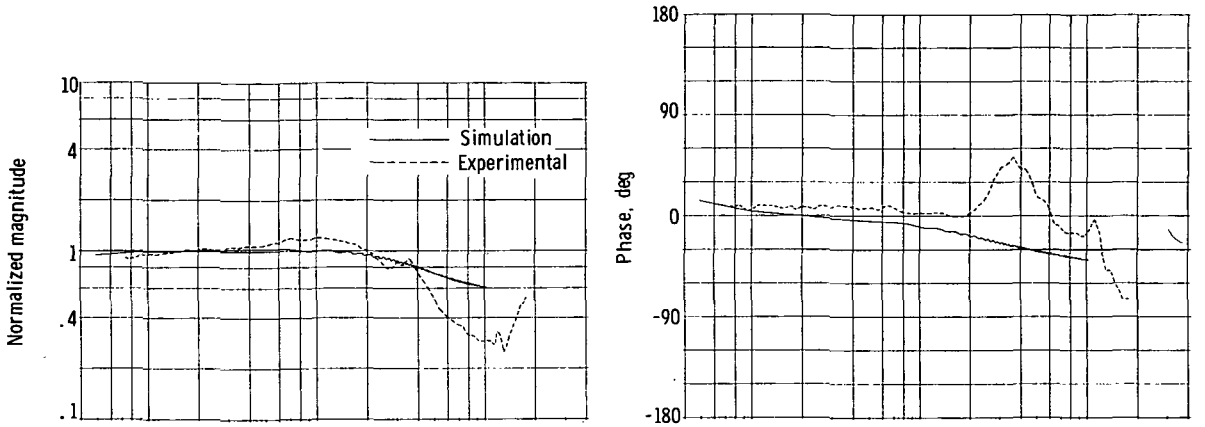


(e) Stage 5 ($P_{t,2.5}/\bar{P}_{t,2}$).

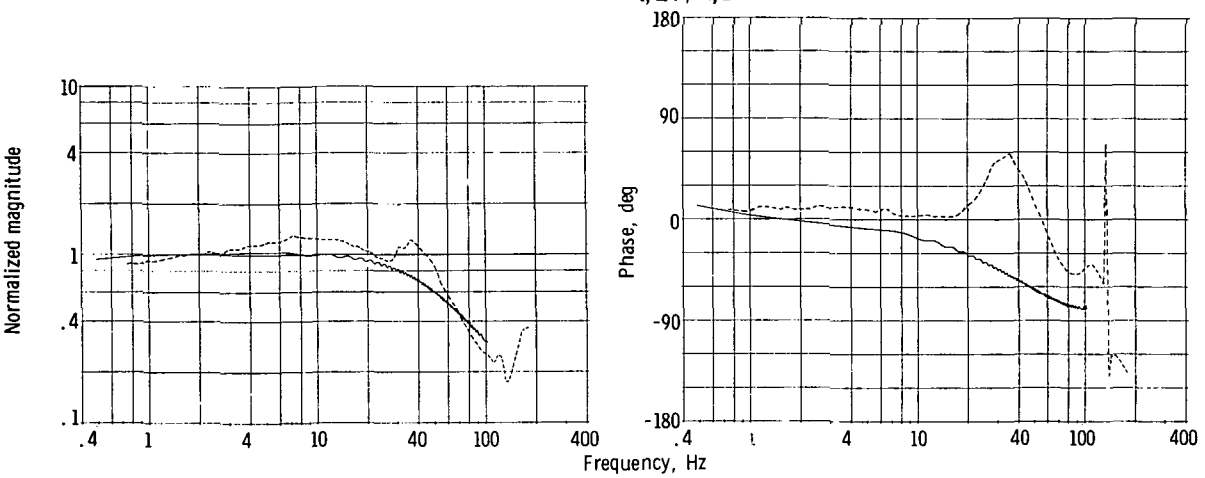


(f) Stage 6 ($P_{t,2.6}/\bar{P}_{t,2}$).

Figure 13. - Continued.



(g) Stage 7 ($P_{t,2.7}/\bar{P}_{t,2}$).



(h) Stage 8 ($P_{t,3}/\bar{P}_{t,2}$).

Figure 13. - Concluded.

NATIONAL AERONAUTICS AND SPACE ADMINISTRATION
WASHINGTON, D.C. 20546

OFFICIAL BUSINESS
PENALTY FOR PRIVATE USE $300

SPECIAL FOURTH-CLASS RATE
BOOK

POSTAGE AND FEES PAID
NATIONAL AERONAUTICS AND
SPACE ADMINISTRATION
451

U.S.MAIL

POSTMASTER : If Undeliverable (Section 158 Postal Manual) Do Not Return

"The aeronautical and space activities of the United States shall be conducted so as to contribute . . . to the expansion of human knowledge of phenomena in the atmosphere and space. The Administration shall provide for the widest practicable and appropriate dissemination of information concerning its activities and the results thereof."

—NATIONAL AERONAUTICS AND SPACE ACT OF 1958

NASA SCIENTIFIC AND TECHNICAL PUBLICATIONS

TECHNICAL REPORTS: Scientific and technical information considered important, complete, and a lasting contribution to existing knowledge.

TECHNICAL NOTES: Information less broad in scope but nevertheless of importance as a contribution to existing knowledge.

TECHNICAL MEMORANDUMS: Information receiving limited distribution because of preliminary data, security classification, or other reasons. Also includes conference proceedings with either limited or unlimited distribution.

CONTRACTOR REPORTS: Scientific and technical information generated under a NASA contract or grant and considered an important contribution to existing knowledge.

TECHNICAL TRANSLATIONS: Information published in a foreign language considered to merit NASA distribution in English.

SPECIAL PUBLICATIONS: Information derived from or of value to NASA activities. Publications include final reports of major projects, monographs, data compilations, handbooks, sourcebooks, and special bibliographies.

TECHNOLOGY UTILIZATION PUBLICATIONS: Information on technology used by NASA that may be of particular interest in commercial and other non-aerospace applications. Publications include Tech Briefs, Technology Utilization Reports and Technology Surveys.

Details on the availability of these publications may be obtained from:

SCIENTIFIC AND TECHNICAL INFORMATION OFFICE

NATIONAL AERONAUTICS AND SPACE ADMINISTRATION

Washington, D.C. 20546